Utilisation of Heat Released During the Production of Green Hydrogen Using Alkaline Electrolysis

F.S. Le Coultre

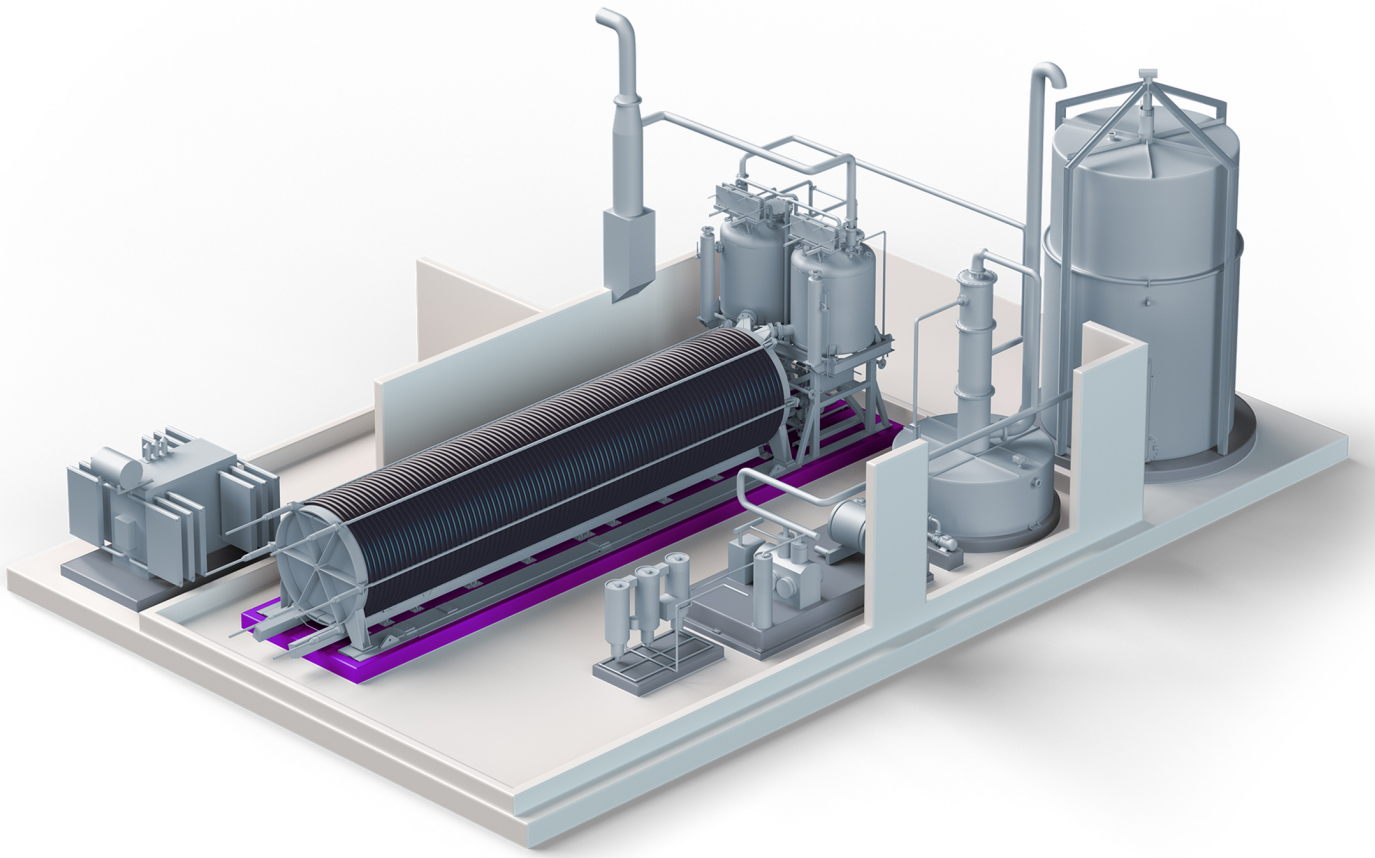

TU Delft Delft University of Technology

alliander

Utilisation of Heat Released During the Production of Green Hydrogen Using Alkaline Electrolysis

by

F.S. Le Coultre

to obtain the degree of Master of Science
at the Delft University of Technology,
to be defended publicly on Monday June 27, 2022 at 14:00 PM.

Student number:	4397037	
Project duration:	August 30, 2021 – June 27, 2022	
Thesis committee:	Dr. ir. R. Kortlever,	Delft University of Technology, supervisor
	Dr. ir. J.W.R. Peeters,	Delft University of Technology, supervisor
	Prof. dr. ir. W. de Jong,	Delft University of Technology
	Ir. M. Houkema,	Alliander

An electronic version of this thesis is available at http://repository.tudelft.nl/.
Cover image retrieved from [1].

TU Delft Delft University of Technology

alliander

Preface

For the last nine months I had the pleasure to learn and study about green hydrogen. I learned much during my time at Qirion and I would like to thank Michiel Houkema for the supervision, his sincere interest in the subject and all the hard questions that forced me to understand and explain my subject better.

I would also like to thank Ruud Kortlever and Jurriaan Peeters for both agreeing to be my supervisors. In my opinion it is really special to have two supervisors from the university who both make time to discuss and supervise my work, providing valuable feedback. Finally, I would like to thank Prof. dr. ir. W. de Jong for being part of my thesis committee.

Florine Le Coultre
Rotterdam, June 2022

Abstract

To reduce greenhouse gas emissions and to limit global warming, fossil fuel based energy technologies need to be replaced by clean energy technologies. Renewable energy sources are dependent on weather conditions therefore security of energy supply is not ensured and the need for energy storage is growing. Hydrogen is considered a clean energy carrier that can be used for energy storage. Water electrolysis that uses renewable energy is a sustainable method for the production of green hydrogen. Water electrolysis is a process by which water is split into hydrogen and oxygen by using direct current to drive the reaction. During the production of green hydrogen heat is released to the environment. Little research has been conducted on the amount of heat released during green hydrogen production and on the temperature of the released heat. It is unclear if the released heat could be used.

This research serves to answer the question "Is it possible to use the heat released during the production of green hydrogen using alkaline water electrolysis?". To answer this question a model has been developed in ASPEN Plus. This model represents an alkaline electrolyser, consisting of an electrochemical model, a thermal model and a cooling system. To validate the output of the model, the hydrogen production output has been compared with an alkaline electrolyser developed by the company Nel hydrogen. The thermal efficiency of the model has been calculated with and without using the waste heat. To use the waste heat the system first needs to be cooled. To determine which heat exchanger is best to use for recovering the heat of the alkaline electrolyser, three different designs have been implemented in the ASPEN model. The designs have been analyzed and the best option is implemented in the model. The amount of heat that can be recovered has been investigated as well as the options for the use of the recovered heat. The results are discussed and recommendations are made for follow-up research.

Contents

1 Motivation **1**

2 Introduction **2**

2.1 Hydrogen production methods & initiatives . . . 2

2.2 Problem statement . . . 5

2.3 Scope & goals . . . 5

3 Literature **7**

3.1 Water electrolysis . . . 7

3.1.1 Alkaline electrolysis . . . 8

3.1.2 Polymer electrolyte membrane (PEM) electrolysis . . . 9

3.1.3 Solid oxide electrolysis . . . 11

3.2 Electrolysis heat loss . . . 12

3.3 Heat recovery . . . 14

3.4 Existing models and limitations . . . 15

4 Method **18**

4.1 ASPEN . . . 18

4.2 Overview model . . . 18

4.2.1 Stack . . . 20

4.2.2 Anodic circuit . . . 23

4.2.3 Cathodic circuit . . . 23

4.3 Electrochemical model . . . 24

4.3.1 Open circuit voltage . . . 26

4.3.2 Activation overpotential . . . 27

4.3.3 Mass transport overpotential . . . 28

4.3.4 Ohmic overpotential . . . 29

4.3.5 Final electrochemical model . . . 30

4.4 Thermal model . . . 30

4.5 Cooling system . . . 32

5 Results and implementation **35**

5.1 Model validation . . . 35

5.2 System efficiency . . . 36
5.3 Cooling system . . . 37
5.4 Heat recovery system . . . 38
5.5 Heat recovered . . . 40
5.6 Heat usage . . . 41

6 Discussion **47**
6.1 Operating temperature . . . 47
6.2 Seasonal effects . . . 48
6.3 Steady state model . . . 49
6.4 Recycle stream . . . 49
6.5 Steady pressure . . . 49
6.6 Input parameters . . . 50

7 Conclusion **51**

8 Recommendations **52**
8.1 Recommendations model . . . 52
8.2 Recommendations topic related research . . . 52

Appendices **61**

A Dutch green hydrogen initiatives **62**

B Heat exchangers **63**

List of Figures

1 Storage Technologies and Power / Energy Characteristics [7]. 2
2 From green energy to green hydrogen: the different production paths [13]. 3
3 Schematic overview hydrogen [14]. 4
4 Total annual production of hydrogen [16][17]. 4
5 Hydrogen projects map worldwide [19]. 5
6 Electrochemical cell [23]. 7
7 Schematic of alkaline electrolyser [36]. 9
8 Schematic of PEM electrolyser [43]. 10
9 Schematic of solid oxide electrolyser [36]. 12
10 Temperature dependence of main thermodynamic parameters for water electrolysis at 1 bar [50]. 14
11 Project Lingen [55]. 16
12 Project GROHW [56]. 16
13 Process model of an alkaline electrolyser in Aspen plus. 19
14 Model input & output. 20
15 Principle of an a) unipolar electrolyser design b) bipolar electrolyser design [62]. 21
16 Stack design in ASPEN for the alkaline electrolyser. 22
17 Flash for separating oxygen and hydrogen. 23
18 Anodic circuit design in ASPEN for the alkaline electrolyser. 23
19 Cathodic circuit design in ASPEN for the alkaline electrolyser. 24
20 Polarisation curve of an alkaline electrolysis cell at 25 °C and 80 °C [65]. 25
21 Overview of the influence of losses on the thermodynamic maximum of an electrolyser [42]. . 25
22 Activation overpotential at 7 bar and 75 °C. 28
23 Ohmic overpotential at 7 bar and 75 °C. 30
24 Heat transfer by (A) heat conduction, (B) heat convection and (C) thermal radiation [74]. . 31
25 Correction factor F_t as a function of NTU (from Sinnott and Towler [80]). 34
26 Produced hydrogen at 7 bar and 75 °C. 35
27 Voltage efficiency as a function of variating temperature and pressure. 36
28 ASPEN model output plate heat exchanger. 37
29 Cooling demand for model operation at 75 °C and 7 bar. 38
30 (a) Forced air HEX [82] (b) Shell & tube HEX [83] (c) Plate HEX [84]. 39
31 (a) Designated surface water bodies (b) Non-designated surface water bodies [87]. 40

32 Energy cooling water stream per hour at system operation of 75 °C and 7 bar. 41
33 Energy cooling water stream per hour predicted at system operation of 75 °C and 7 bar. . . 41
34 Medium heat network projects in the Netherlands [89]. 43
35 Heat for households considering 25 % losses for transportation. 44
36 ASPEN model with shell & tube HEX for swimming pool. 45
37 The influence of temperature on E_{cell}. 47
38 Seasonal fluctuations air temperature the Netherlands and the influence on the flowrate for the cooling of an alkaline electrolyser stack consisting of 12 stacks of cells [95]. 48
39 Seasonal fluctuations water temperature of the North sea and the influence on the flowrate for the cooling of an alkaline electrolyser stack consisting of 12 stacks of cells [96]. 48
40 The influence of pressure on E_{cell}. 49
41 Sensitivity curve: influence of changing duty on temperature cool water stream. 50
42 ASPEN model output air cooled heat exchanger. 63
43 ASPEN model output shell & tube heat exchanger. 64
44 ASPEN model output shell & tube heat exchanger tubesheet layout. 65

List of Tables

1 Main specifications of an alkaline electrolyser [37][38][39][40]. 9

2 Main specifications of a PEM electrolyser [37][38][39][40]. 11

3 Main specifications of a solid oxide electrolyser [37][38][39][40]. 12

4 Model inputs. 20

5 Conditions of the flows. 33

6 Volume flow H_2 output stream. 36

7 Heat exchangers implemented in the ASPEN model. 39

8 Low temperature heating [88]. 42

9 Shell & tube HEX implemented in the ASPEN model for air-water heating for a swimming pool. 45

10 Dutch green hydrogen production initiatives [20]. 62

Nomenclature

Abbreviations

ATR	Autothermal Reforming
CCS	Carbon Capture & Storage
HER	Hydrogen Evolution Reaction
HHV	Higher Heating Value
OCV	Open Circuit Voltage
OER	Oxygen Evolution Reaction
PEM	Polymer Electrolyte Membrane
SMR	Steam Methane Reforming
$SOEC$	Solid Oxide Electrolyser
ACM	ASPEN Custom Modeler
ORC	Organic Rankine Cycle
COP	Coefficient Of Performance
HEX	Heat Exchanger
EDR	Exchanger Design and Rating

Symbols

α_a	Anodic transfer coefficient	[-]
α_c	Cathodic transfer coefficient	[-]
$\Delta G(T)$	Gibbs free energy change	[J/mol]
ΔG^0_{T}	Gibbs free energy change under standard conditions	[J/mol]
$\Delta H(T)$	Change of enthalpy	[J/mol]
$\Delta S(T)$	Entropy change	[J/mol/K]
ΔT_{lm}	Log mean temperature difference	[K]
δ	Boundary layer thickness	[m]
$\dot{\mathrm{Q}}$	Heat transfer rate	[W]
$\dot{m}_{cw}$	Cooling water mass flowrate	[kg/s]
$\dot{Q}_{\mathrm{evap}}$	Thermal demand evaporation	[W]
$\dot{Q}_{cond}$	Thermal demand conduction	[W]

$\dot{Q}_{conv}$	Thermal demand convection	[W]
$\dot{Q}_{cool}$	Cooling	[W]
$\dot{Q}_{gen}$	Generated heat	[W]
$\dot{Q}_{loss}$	Lost heat	[W]
$\dot{Q}_{rad}$	Thermal demand radiation	[W]
$\dot{Q}_{renov}$	Thermal demand renewed water	[W]
$\dot{Q}_{tot}$	Total thermal power demand	[W]
$\dot{W}_{\mathrm{loss}}$	Heat loss	[W]
η_{act}	Activation overpotential	[V]
η_{ohm}	Ohmic & ionic overpotential	[V]
η_{stack}	Efficiency of stack	[-]
η_{system}	System efficiency	[-]
η_{thermo}	Thermoneutral (voltage) efficiency	[-]
η_{trans}	Mass transport overpotential	[V]
$\frac{dT}{dx}$	Temperature gradient	[K/m]
ρ	Density	[kg/m^3]
σ	Stefan-Boltzmann constant	5.669×10^{-8} [W̃ / m^2 K^4]
ε	Emissivity of the surface	[-]
A	Area	[m^2]
a	Activity coefficient	[-]
C_i	Concentration gradient	[mol/m^{-3}]
C_{pcw}	Specific heat of cooling water	[J/kgK]
C_{Bulk}	Bulk concentration	[m^{-3}]
$C_{i,mem,0}$	Reference concentration	[mol/m^{-3}]
$C_{i,mem}$	Concentration of species i at membrane electrode interface	[mol/m^{-3}]
C_p	Specific heat	[J/kg K]
$COP_{heating}$	Coefficient of performance for heating	[-]
$d1$	Constant	3.12996*10^{-6}[Ω m^2]
$d2$	Constant	4.47137*10^{-7}[Ω m^2 bar^{-1}]
D	Diffusion coefficient	[m^2 s]

$Duty_{stack}$	All energy put into stack	[W]
$Duty_{system}$	All energy put into system	[W]
E	Open ciruit voltage	[V]
e^-	Electron	$-1.602176634 \times 10^{-19}$ [C]
E^0	Equilibrium potential	[V]
E_b	Total emissive power	[W/m^2]
E_{cell}	Overall cell potential	[V]
E_{rev}	Reversible cell potential	[V]
F	Faraday constant	96485 [C/mol]
F_t	Correction factor	[-]
G	Irradiation	[W/m^2]
H^+	Proton	$1.602176634 \times 10^{-19}$ [C]
I	Current	[A]
i	Current density	[A/m^2]
i_0	Exchange current density	[A/m^2]
i_L	Limiting current density	[A/m^2]
$i_{0,a}$	Anodic exchange current density	[A/m^2]
$i_{0,c}$	Cathodic exchange current density	[A/m^2]
J	Diffusion flux	[mol/(m^2 s)]
k	Thermal conductivity	[W/(m K)]
k_m	Mass transfer coefficient	[m/s]
N	Number of cells	[-]
n	Amount of electrons transferred	[-]
NTU	Number of transfer units	[-]
P_{xx}	Partial pressure	[atm]
Q	Heat content	[J]
q	Heat flow	[W]
Q_{irrev}	Irreversible heat	[W]
Q_{rev}	Reversible heat	[W]
$r1$	Constant	4.45153*10^{-5} [Ω m^2]

$r2$	Constant	$6.88874*10^{-9}$ [Ω m^2 °C^{-1}]
R	Absolute gas constant	8.314 [J/mol/K]
R	Resistance	[Ω]
s	Constant	0.33824[V]
SH	Sherwood constant	[-]
$t1$	Constant	0.01539[m^2 A^{-1}]
$t2$	Constant	2.00181[m^2 °C A^{-1}]
$t3$	Constant	15.24178[m^2 °C^2 A^{-1}]
T	Temperature	[K]
T_1	Sink temperature	[K]
T_2	Source temperature	[K]
T_C	Input temperature	[K]
T_H	Output temperature	[K]
T_m	Corrected mean temperature	[K]
$T_{\mathrm{cw,in}}$	Cooling water input temperature	[K]
$T_{\mathrm{cw,out}}$	Cooling water output temperature	[K]
U_{0ass}	Estimated overall heat transfer coefficient	[W/m^{2}K]
V	Flowrate	[m^3/s]
W	Work	[J]

1 Motivation

Climate change and an increase in extreme weather events have caused a surge in natural disasters. Climate and weather related disasters have surged five-fold over the last 50 years as a result of global warming [2]. To reduce greenhouse gas emissions and to limit global warming, fossil fuel based energy technologies need to be replaced by clean energy technologies.

Changing to clean energy technologies, however, is a challenge for several reasons. Firstly, renewable energy sources like wind and solar are dependent on weather conditions and do not produce consistently. Therefore, security of energy supply is not ensured. Secondly, electrification is considered the best way to decarbonize the energy system according to the EU. Yet, the current electricity network is not built to transport such high amounts of electricity and therefore net congestion is a problem. Lastly, the world energy consumption increased from 8 x 10^{12} kWh/yr in 1860 to 173 x 10^{12} kWh/yr in 2019. Approximately 137 x 10^{12} kWh/yr (79 %) is produced by fossil fuels (coal, oil and gas) [3][4]. This means that the world energy consumption in the last 159 years has multiplied by a factor of 22. To summarize, the goal is to limit global warming using renewable energy sources. The focus lies on electrification to decarbonize the energy system although net congestion is already a problem. Next to this, the world energy demand is rising fast, while security of energy supply is not ensured since renewable energy sources are dependent on weather conditions.

The solution to overcome these problems is energy storage. Numerous possibilities for storage are currently being researched and implemented. Power-to-gas is one of the storage possibilities. The power-to-gas method uses electricity to produce a gas. This gas is an energy carrier. Therefore, when burning this gas the electricity is released and can be used. Different gasses can be used for power-to-gas like hydrogen or methane. For the production of hydrogen, methods can be used which are considered free of CO_2 emissions. There is much interest in the possibilities to produce and use hydrogen as energy carrier. Therefore, the company Qirion wants to know more about the production of green hydrogen and the heat that gets released during this process.

Qirion, part of the company Alliander, designs, builds and maintains the energy grid of today and tomorrow and makes sure it works. A part of Qirion is Qirion Energy Consulting. Qirion Energy Consulting helps customers to invest in new, open networks such as heat and hydrogen networks. Qirion energy consulting is characterized by the use of knowledge and experience in various energy areas. They innovate, advise, design and realize integral sustainable energy systems and energy concepts.

As part of Qirion, this work serves to investigate and learn more about the production of green hydrogen using water electrolysis and to look more in depth into the generation of heat that gets released during alkaline electrolysis. The knowledge retrieved from this research is used for recommendations to future clients of Qirion.

2 Introduction

Hydrogen or H_2 is considered a clean energy carrier. Currently, hydrogen is mainly used as chemical in many industrial processes instead of as energy carrier. In 2018 the global demand for hydrogen was equal to 73.8 Mt. The largest part of this amount was used for refining and ammonia, but hydrogen is used in many different markets for example in the aerospace industry [5]. However, hydrogen could also be useful in combination with renewable energy systems. At times when there is more electricity than is needed, it is possible to produce hydrogen with the abundant electricity. In times when there is need for more electricity, the hydrogen can be used to produce electricity again. As a result, the energy system is flexible and the security of energy supply can be ensured [6]. The energy storage capacity of a power-to-gas hydrogen system is considered one of the biggest compared to other energy storage technologies as can be seen in figure 1.

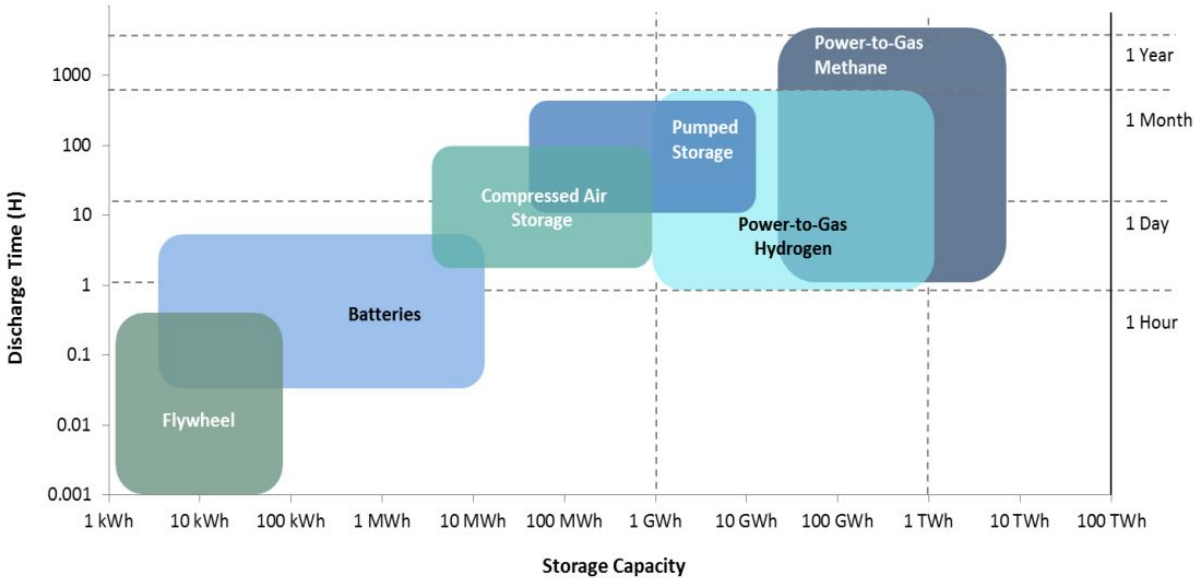

Figure 1: Storage Technologies and Power / Energy Characteristics [7].

Thus, hydrogen is expected to help reach security of energy supply in the electricity market because of its possibilities for electricity storage [8]. Hydrogen gas has the highest higher heating value (HHV) per kilogram compared to common used gaseous fuels. 324 g of hydrogen has the same energy content as 1 kg gasoline. However, the energy content of hydrogen per volume is only a quarter of the energy density of gasoline. The volumetric energy density of hydrogen can be increased by compression or liquefaction [9].

2.1 Hydrogen production methods & initiatives

There are different ways to produce hydrogen. Depending on the production method, hydrogen is either denoted as grey, blue or green hydrogen. The most commonly produced is grey hydrogen. Grey hydrogen is produced using fossil resources. Steam methane reforming (SMR) or autothermal reforming (ATR) of natural gas is used for the production of grey hydrogen [10]. In total, about 6 % of global natural gas production and 2 % of global coal production is used to make approximately 70 Mt of hydrogen per annum. This results in atmospheric emissions of about 830 Mt of carbon dioxide [5]. That is more than Germany emitted in 2016 [11]. Blue hydrogen, also known as low-carbon hydrogen, is produced in the same way as

grey hydrogen but makes use of carbon capture and storage (CCS) [12]. As a result blue hydrogen emits less CO_2 than grey hydrogen. When using grey or blue hydrogen, the goal of being climate neutral by the time of 2050 will not be possible because these methods still emit green house gasses such as CO_2. Green hydrogen is made using renewable energy sources and can be seen as a clean way to produce hydrogen. The forms of energy needed to produce hydrogen from natural resources can be classified in four categories, namely thermal, electrical, photonic and biochemical. The hydrogen production process can be called green when the energy needed comes from green energy sources [13]. An overview of all the different possibilities can be seen in figure 2.

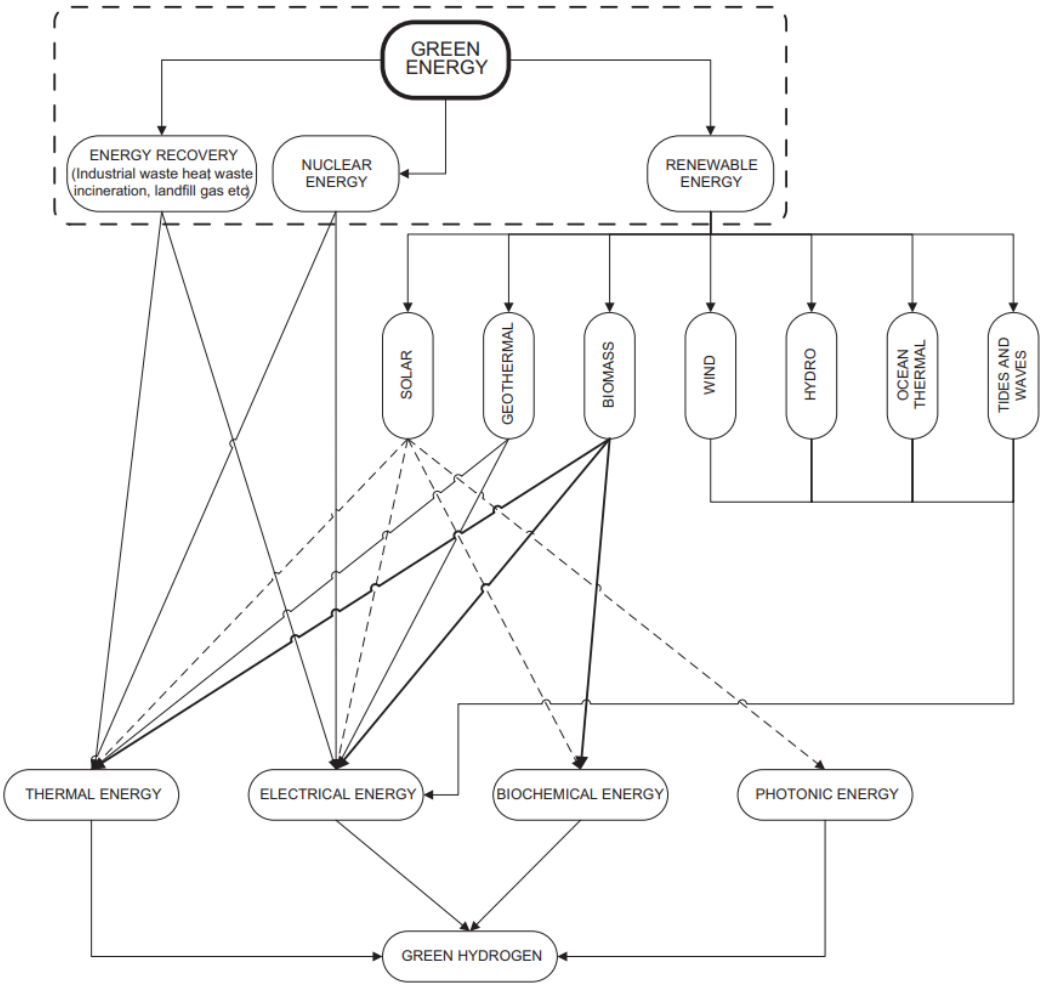

Figure 2: From green energy to green hydrogen: the different production paths [13].

Different energy sources have different hydrogen production methods. For example, when making use of thermal energy the hydrogen production method thermolysis is used. There are many different green hydrogen production methods. The most commonly used method is water electrolysis. Water electrolysis makes use of electrical energy and uses water to produce hydrogen. In figure 3 a schematic overview of the production of hydrogen using water electrolysis is shown.

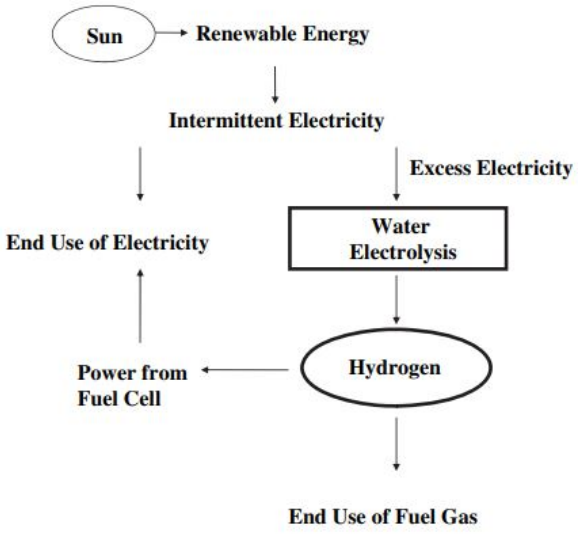

Figure 3: Schematic overview hydrogen [14].

Currently, water electrolysis is not used as often as other methods for the production of hydrogen. This is shown in figure 4. Only 4 % of produced hydrogen is produced by electrolysis with a total amount of 20 billion cubic meters. A reason for this is the cost of the production of hydrogen by electrolysis. The production of green hydrogen has always been more expensive than the production of hydrogen using fossil resources. The goal is to change this, due to larger scale and more research. However, the price of green hydrogen is already lower than the price for grey hydrogen due to the high gas prices [15].

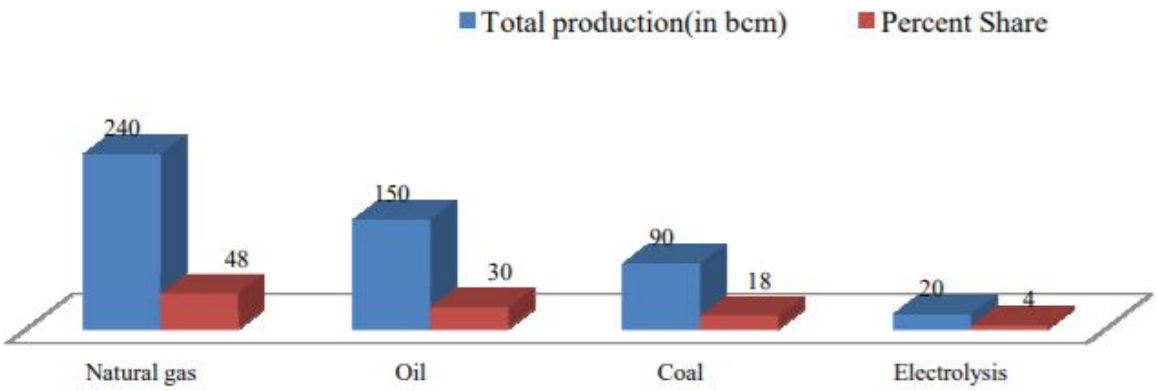

Figure 4: Total annual production of hydrogen [16][17].

Many countries are acknowledging that hydrogen is needed in the future and therefore new green hydrogen projects are started every month. One of these projects is called HyDeal ambition. 30 energy players initiate and integrate a value chain to deliver green hydrogen across Europe at the price of fossil fuels. The ambition is to achieve 95 GW of solar power, coming from the Iberian Peninsula and 67 GW of electrolysis capacity by 2030 to deliver 3.6 million tonnes of green hydrogen per year to users. At the moment, this is the largest hydrogen initiative worldwide [18]. In figure 5 the biggest green hydrogen projects in the world are mapped out.

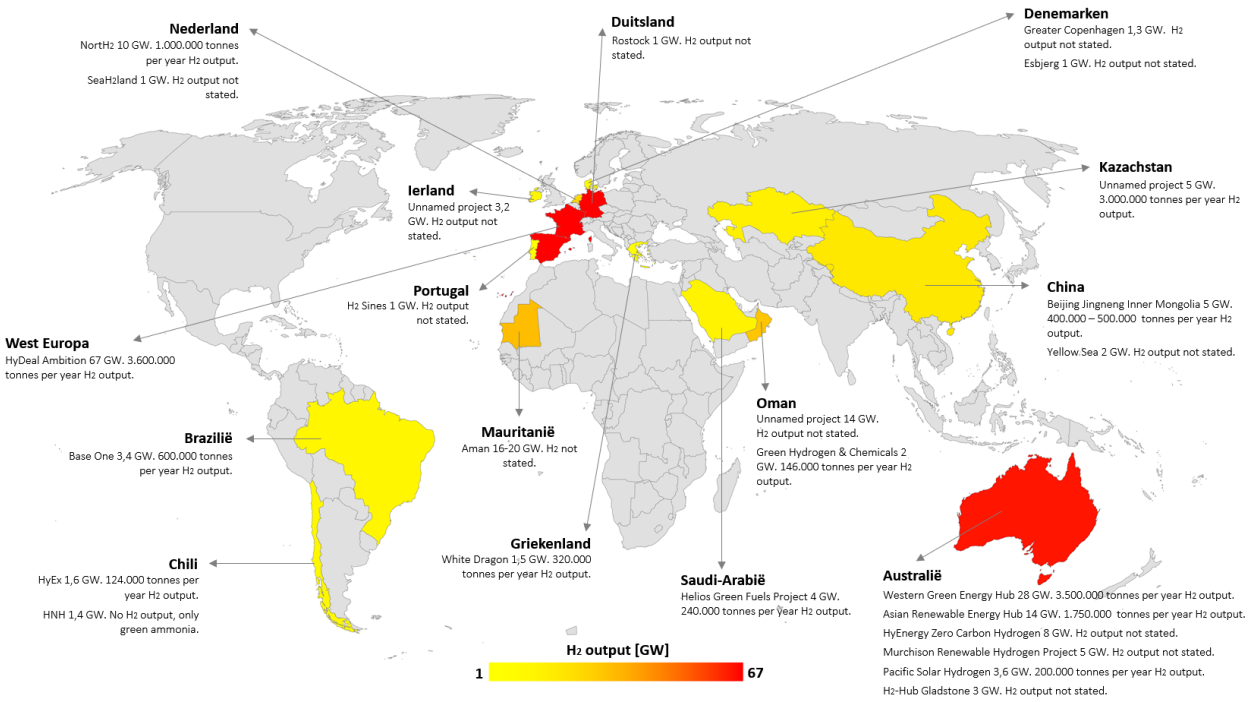

Figure 5: Hydrogen projects map worldwide [19].

In the Netherlands, the production of green hydrogen is also starting to bloom. Currently, over 35 projects for the production of green hydrogen in the Netherlands are being developed. The biggest being NorthH2. The objective of NorthH2 is to generate 3 to 4 GW of wind energy for hydrogen production by 2030, and possibly 10 GW in 2040. The output will be a green hydrogen production of 800.000 tons, which leads to a prevention of around 7 megatons of CO_2 emissions per year [20]. In appendix A several green hydrogen production projects are shortly mentioned.

2.2 Problem statement

When producing green hydrogen, oxygen and heat are produced as by-products and released into the environment. In 2018 50 % of global final energy consumption consisted out of heat. Thermal energy is responsible for 40 % of the global carbon dioxide (CO_2) emissions. Fossil fuels continue to dominate heat supplies, while modern renewables (i.e. excluding the traditional use of biomass) met only 10 % of global heat demand in 2018 [21]. In short, efficient use of the readily available heat is required. Therefore, the heat and oxygen produced during the production of green hydrogen can better be used than wasted. The oxygen could be used in sewage treatment plants. The average oxygen demand of a medium size sewage treatment plant is equal to 4468 ton CO_2 per year according to numbers of Qirion. The heat could be used for district heating among others. Using the by-products originated from water electrolysis could increase the efficiency and lower the costs.

2.3 Scope & goals

This study serves to understand and learn more about the production of green hydrogen using water electrolysis and to look more in depth into the generation of heat that gets released during electrolysis. The

possibility of using the excess heat will be investigated on the basis of the following research question and subquestions.

Research question:
Is it possible to use the heat released during the production of green hydrogen using alkaline water electrolysis?

Subquestions:

- How much heat does an alkaline electrolyser produce when producing green hydrogen?
- How much of the heat can, in theory, be recovered from the process?
- What is the temperature of the heat recovered from the process?
- What heat recovery system can best be used to recover the heat?
- What possible applications are there for the use of the excess heat?
- Which of the possible applications for the use of the excess heat is considered most profitable and why?

To answer the research question and corresponding subquestions a model of an alkaline electrolyser has been built in ASPEN. First, in chapter 3, literature is presented on the background of the problem. In chapter 4 the different models, which together form the alkaline electrolyser, are presented. In chapter 5 the results of the model are presented and the model is verified. The type of heat exchanger is determined that needs to be used for the model to retrieve the optimal output as well as how much heat can be used and for what purposes. This is followed by a brief discussion. In chapter 7 the conclusion is presented followed by recommendations for follow-up research.

3 Literature

3.1 Water electrolysis

Water electrolysis is a process by which water is split into hydrogen and oxygen. In figure 6 an electrochemical cell is shown. In an electrochemical cell energy arises by a spontaneous redox reaction. This energy is converted into electricity. These chemical reactions take place in a solution at the interface of an electron conductor (a metal or a semiconductor) and an ionic conductor (the electrolyte). It involves electron transfer between the electrode and the electrolyte or species in the solution. In theory, an electrochemical cell can support any reaction performed with the use of ions. The requirement is in availability of an electrolyte transporting those ions [22].

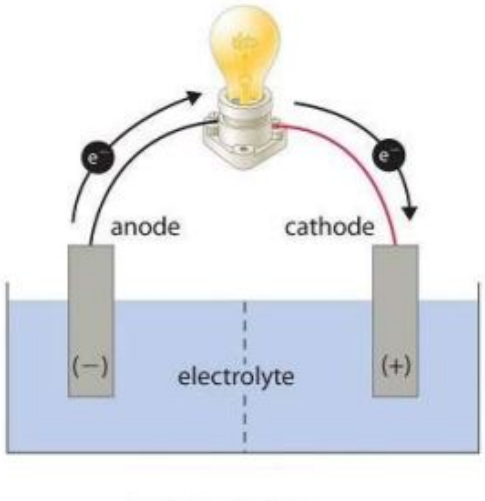

Figure 6: Electrochemical cell [23].

A reaction where electrons are transferred from one reactant to another is called a redox reaction. When a reactant loses electrons, the oxidation state becomes more positively charged. Loss of electrons by a substance is called oxidation (equation 1). When a reactant gains electrons it becomes more negatively charged. The gain of electrons by a substance is called reduction (equation 2).

$$\mathrm{Y} \rightarrow \mathrm{Y}^{+} + \mathrm{e}^{-} \tag{1}$$

$$Z^{+} + e^{-} \rightarrow Z \tag{2}$$

The oxidation half reaction and the reduction half reaction together give the overall cell reaction which is shown in equation 3.

$$\mathrm{Y} + \mathrm{Z} \rightarrow \mathrm{Y}^{+} + \mathrm{Z}^{-} (G < 0) \tag{3}$$

In an electrochemical cell the oxidation reaction takes place on the anode and the reduction reaction takes place on the cathode. Both compartments are chemically separated but electrically connected [23].

Liquid water can be split into its elemental components hydrogen and oxygen according to equation 4 [24].

$$H_2O(l) \rightarrow H_2(g) + \frac{1}{2}O_2(g) \tag{4}$$

This reaction does not occur spontaneously. This is where water electrolysis comes in. Water electrolysis is a method that uses direct current to drive the reaction in equation 4. The water electrolysis process occurs through two simultaneously occurring half cell reactions namely, the oxygen evolution reaction (OER) on the anode and the hydrogen evolution reaction (HER) on the cathode. The oxygen evolution reaction kinetics are slower than the hydrogen evolution reaction kinetics. Therefore, the performance of water electrolysers heavily depends on the oxygen evolution reaction [25][26]. The water molecule passes through an electrochemical process. Pure water is a very poor conductor of electricity. To improve the conductivity an acid or base is used [16]. In a device which consumes power, the cathode is negative and in a device which provides power, the cathode is positive. Usually negative charges move towards the anode. The anode is positive in a device that consumes power, and the anode is negative in a device that provides power [16]. The hydrogen obtained by electrolysis has a high purity that can reach 99.999 vol.% once the produced hydrogen has been dried and oxygen impurities have been removed. The electrolytic hydrogen is suitable for being directly used in low-temperature fuel cells [27]. The purity of water can be a concern in water electrolysis. The presence of metal atoms in water such as calcium or magnesium can cause reactions at the electrode surface that eventually lead to scale formation, consequently reducing the active surface area and enhancing clogging of the diaphragm. The salinity of water is important; if water contains NaCl, or other sources of chlorine ions, chlorine gas will emanate at the cathode with a highly corrosive effect [28].

For the production of green hydrogen different types of electrolysers can be used. Every electrolyser has different characteristics and efficiencies. The efficiency of electrolysers can be described in different ways, such as the stack efficiency, voltage efficiency, overall efficiency, energy efficiency and water to hydrogen conversion efficiency [29]. The two electrolysers that are used commercially are the alkaline water electrolyser and the polymer electrolyte membrane electrolyser. A third is the solid oxide electrolyser. This electrolyser is not yet commercially available but is considered to have high potential. In the following sub chapters the different electrolysers are being discussed.

3.1.1 Alkaline electrolysis

Alkaline electrolysis uses a liquid electrolyte, with high concentrations of potassium hydroxide to provide ionic conductivity and to participate in the electrochemical reactions [30]. The oxidation and reduction reactions used in an alkaline electrolyser are shown in equation 5 & 6.

$$\text{Anode}: \ 2OH^- \rightarrow \frac{1}{2}O_2 + H_2O + 2e^- \tag{5}$$

$$\text{Cathode}: \ H_2O + 2e^- \rightarrow 2OH^- + H_2 \tag{6}$$

In an alkaline electrolyser the liquid electrolyte consists of a high concentration of KOH (25-35 wt%) in water. NaOH can also be used as electrolyte media. The charge carrier is the hydroxide ion OH^- [31]. The cell operates at a temperature of $< 80°C$ [32]. An alkaline environment makes the oxygen evolution reaction easier. Therefore, the use of noble materials for the electrocatalyst is not needed which leads to a price advantage. In alkaline electrolysis, the most commonly used anode and cathode materials are nickel- and cobalt-based oxides [33]. One of the main disadvantages of alkaline electrolysis is the low operational current density. When the current density increases, the typical cell voltage also increases. The typical cell voltage

in an alkaline electrolyser lies between 1.8-2.4 V. At this value the operational current density for alkaline electrolysis is equal to 0.6 A/cm^2 which is considered low. As a result, the efficiency of the system is lower than when having high operational current densities [34, 35]. In figure 7 a schematic overview of an alkaline electrolyser cell is shown. In table 1 the values of the main specifications of an alkaline electrolyser are shown.

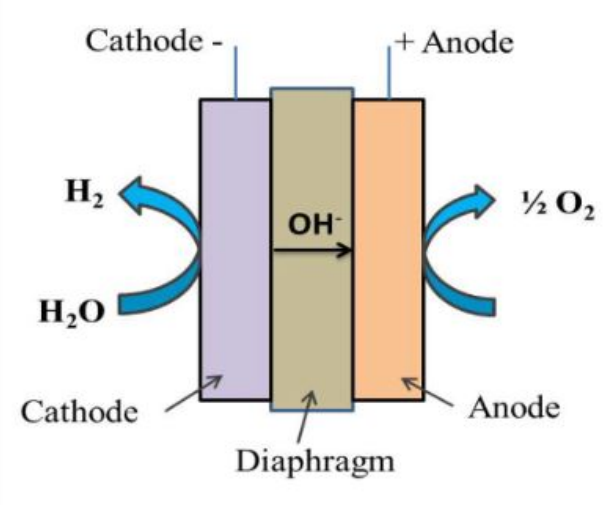

Figure 7: Schematic of alkaline electrolyser [36].

Table 1: Main specifications of an alkaline electrolyser [37][38][39][40].

Specification	**Value**
Operating Temperature [°C]	60-90
Operating Pressure [bar]	2-10
Cell Voltage [V]	1.8-2.4
Current Density [A/cm^2]	0.2-0.4
Voltage Efficiency [%]	62-82
H_2 Capacity [Nm^3/h]	<760
Lifetime of the Stack [h]	<90.000
Lifetime of the System [year]	20-30
Cold Start-Up Time [minutes]	<60
System Energy Consumption [kWh/Nm^3]	>4.5-7

Alkaline electrolysis is a simple and old technology. The main advantage of alkaline electrolysis is the suitability for large hydrogen demand. It is one of the easiest, simplest and most suitable methods for hydrogen production. Disadvantages of alkaline electrolysis are the problems of relatively high energy consumption, installation costs, maintenance costs, durability and safety [41][42].

3.1.2 Polymer electrolyte membrane (PEM) electrolysis

In polymer electrolyte membrane (PEM) water electrolysis, water is electrochemically split into hydrogen and oxygen at their respective electrodes such as hydrogen at the cathode and oxygen at the anode. In PEM

water electrolysisis water is being pumped to the anode where it is spilt into oxygen (O_2), protons (H^+) and electrons (e^-). These protons travel via a proton conducting membrane to the cathode side. The electrons exit from the anode through the external power circuit, which provides the driving force (cell voltage) for the reaction. At the cathode side the protons and electrons re-combine to produce the hydrogen [36]. A schematic overview of a PEM electrolyser is shown in figure 8.

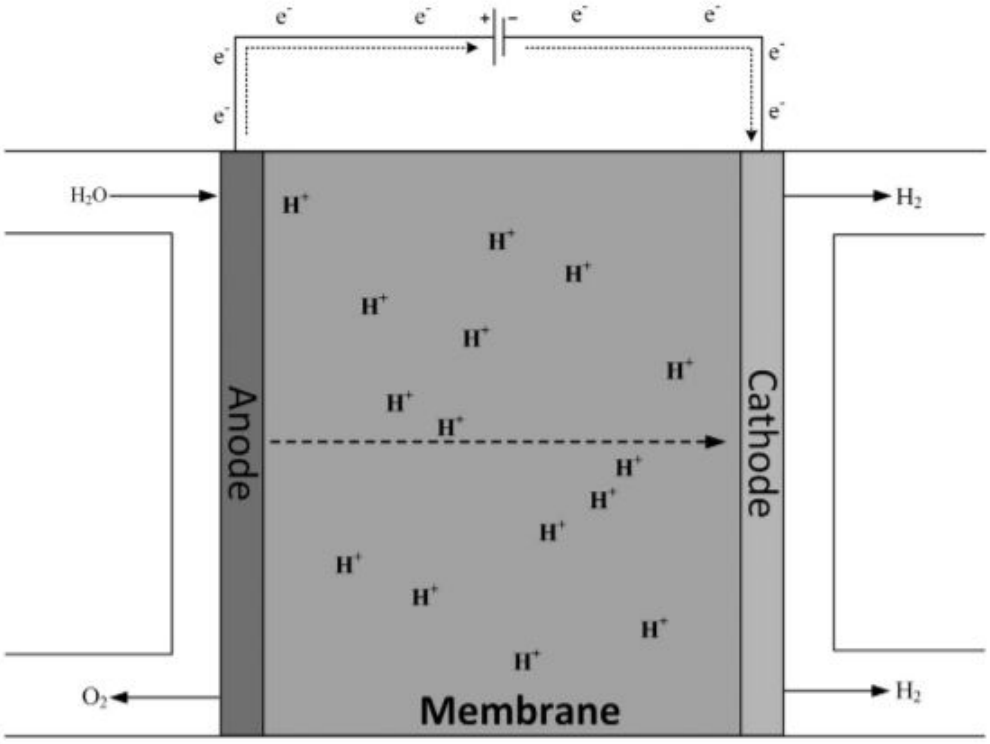

Figure 8: Schematic of PEM electrolyser [43].

PEM electrolysis shows the best performance for hydrogen generation. However, huge hydrogen plants will be required to satisfy the demand of hydrogen. PEM electrolysis would face real difficulty in satisfying such a large requirement because the translation of catalyst development from lab scale to megawatt scale remains challenging in terms of catalyst cost and stability. [44] [41]. PEM electrolysis replaces the liquid electrolyte with a solid polymer electrolyte, which selectively conducts positive ions such as protons. The protons participate in the water-splitting reaction instead of hydroxide, creating a locally acidic environment in the cell [30]. Electrolysers using a liquid acidic electrolyte are not common because of severe corrosion issues [45]. In equation 7 & 8 the half reactions that occur in the PEM electrolyser are shown.

$$\text{Anode}: \ H_2O \rightarrow 2H^+ + \frac{1}{2}O_2 + 2e^- \tag{7}$$

$$\text{Cathode}: \ 2H^+ + 2e^- \rightarrow H_2 \tag{8}$$

As can be concluded from the half reactions, the charge carrier in a PEM electrolyser is the H^+ ion (proton). In table 2 the values of the specifications of a PEM electrolyser are shown. As mentioned earlier, PEM electrolysers can operate at higher current densities than alkaline electrolysers. An advantage of the PEM

electrolyser is the relatively low starting time compared to the other electrolysers. A disadvantage of the PEM electrolyser is the high costs caused by the precious materials needed for the catalyst and the membrane [46].

Table 2: Main specifications of a PEM electrolyser [37][38][39][40].

Specification	**Value**
Operating Temperature [°C]	50-90
Operating Pressure [bar]	15-30
Cell Voltage [V]	1.8-2.2
Current Density [A/cm^2]	0.6-2.0
Voltage Efficiency [%]	67-82
H_2 Capacity [Nm^3/h]	<40
Lifetime of the Stack [h]	<20.000
Lifetime of the system [year]	10-20
Cold start-up time [minutes]	<20
System Energy Consumption [kWh/Nm^3]	>4,5-7,5

3.1.3 Solid oxide electrolysis

Different from alkaline and PEM electrolysis, a solid oxide electrolyser (SOEC) works at temperatures in the range of 500-1000 °C. The high temperature electrolysis is favorable due to its thermodynamics. At high temperatures the overall voltage needed to drive the water splitting reaction lowers and therefore, the total electricity demand decreases significantly compared to the rise in thermal energy demand [47]. Ionic conductivity of the electrolyte and rates of electrochemical reactions at the electrode surfaces increases at high temperature [16]. The half reactions that take place in a SOEC are shown in equation 9 & 10.

$$\text{Anode}: \ O^{2-} \rightarrow \frac{1}{2}O_2 + 2e^- \tag{9}$$

$$\text{Cathode}: \ H_2O + 2e^- \rightarrow H_2 + O^{2-} \tag{10}$$

In SOEC O^{2-} functions as the charge carrier. The key components of a SOEC are a dense ionic conducting electrolyte and two porous electrodes. Steam is fed to the porous cathode. When required electrical potential is applied to the SOEC, water molecules diffuse to the reaction sites and are dissociated to form hydrogen gas and oxygen ions at the cathode–electrolyte interface. The hydrogen gas produced diffuses to the cathode surface and gets collected. The oxygen ions are transported through the dense electrolyte to the anode. On the anode side, the oxygen ions are oxidized to oxygen gas and the produced oxygen is transported through the pores of the anode to the anode surface [48]. A schematic overview of a solid oxide electrolyser cell is shown in figure 9.

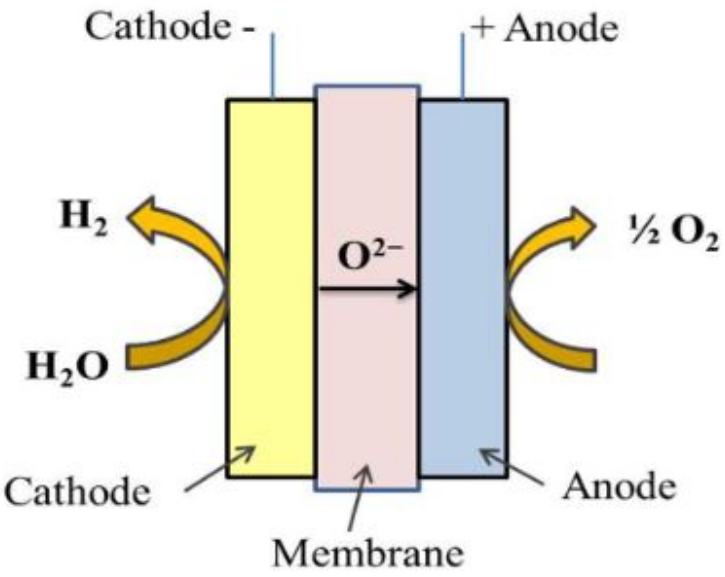

Figure 9: Schematic of solid oxide electrolyser [36].

SOEC is still in the demonstration phase and is not used commercially yet, although it is considered to have high potential. In table 3 an overview of the specifications and values of a SOEC are shown. The biggest advantages of the SOEC are the low electricity need, low capital costs and high efficiency. The capital costs are low as a result of the absence of a membrane and a catalyst of precious materials. Research is still being done since the electrolyser is experiencing safety problems, has an unsuitable sealing and is missing electrode stability.

Table 3: Main specifications of a solid oxide electrolyser [37][38][39][40].

Specification	**Value**
Operating Temperature [°C]	500-1000
Operating Pressure [bar]	<30
Cell Voltage [V]	0.7-1.5
Current Density [A/cm^2]	0.3-1.0
Voltage Efficiency [%]	81-86
H_2 Capacity [Nm^3/h]	<40
Lifetime of the Stack [h]	<40.000
Lifetime of the System [year]	-
Cold Start-Up Time [minutes]	<60
System Energy Consumption [kWh/Nm^3]	>3.7

3.2 Electrolysis heat loss

Assuming that the chemical reaction, needed for the water splitting reaction, is performed along a reversible path and under isothermal conditions the following relation holds:

$$\Delta G(T) = \Delta H(T) - T\Delta S(T) \tag{11}$$

Where $\Delta S(T)$ is the entropy change in J/mol/K, $\Delta H(T)$ is the enthalpy of the reaction in J/mol and $\Delta G(T)$ is the Gibbs free energy change in J/mol. The Gibbs free energy change represents the amount of electricity that has to be supplied to the electrolysis cell to dissociate water [45].

During electrolysis, heat is created because an overpotential is applied to the electrochemical cell. An overpotential is the difference between the theoretical cell voltage and the actual voltage that is necessary to drive electrolysis [49]. The theoretical cell voltage and the actual voltage are not equal due to losses and resistances in the water electrolysis process. These losses and resistances are mainly dependent on the characteristics of the electrochemical cell. Under standard conditions, the Gibbs free energy change required for the electrolysis of 1 mol of water is equal to the following equation:

$$\Delta G_{\mathrm{T}}^{0} = nFE^{0} \tag{12}$$

E^0 is the equilibrium potential in V and is equal to 1.229 V. When a cell voltage of less than 1.229 V is applied to the electrolysis cell, nothing happens. There is not enough energy supplied to perform the non-spontaneous reaction. The thermoneutral voltage is the voltage required for water electrolysis to occur at constant temperature and therefore without the exchange of heat to the surroundings. The value of the thermoneutral voltage is dependent on the change in Gibbs free energy and, therefore, temperature dependent. At temperatures less than 100 °C the value of the thermoneutral voltage will be equal to 1.48 V and slightly depends on pressure. When the cell voltage is lower than 1.48 V electrolysis is possible, but heat needs to be supplied from the surroundings. When the cell voltage is higher than 1.48 V the electrolysis process is exothermic and heat is released to the surroundings [45]. How much heat is released is dependent on the cell potential (V), the reversible cell potential (V) and the current (A). The relationship is shown in equation 13. Where $\dot{W}_{\mathrm{loss}}$ represents the heat loss in W.

$$E_{cell} I = E_{\mathrm{rev}}\, I + \dot{W}_{\mathrm{loss}} \tag{13}$$

The reversible cell potential is defined in equation 14 [28].

$$E_{\mathrm{rev}} = -\frac{\Delta G}{nF} \tag{14}$$

It is also possible to produce hydrogen at higher temperatures. In figure 10 it can be seen that at higher temperatures more heat is needed, but less electrical energy. Since the cost for 1 kWh of heat is substantively lower than the price of 1 kWh of electricity, the energy cost for splitting water into hydrogen is less expensive at higher temperatures [45].

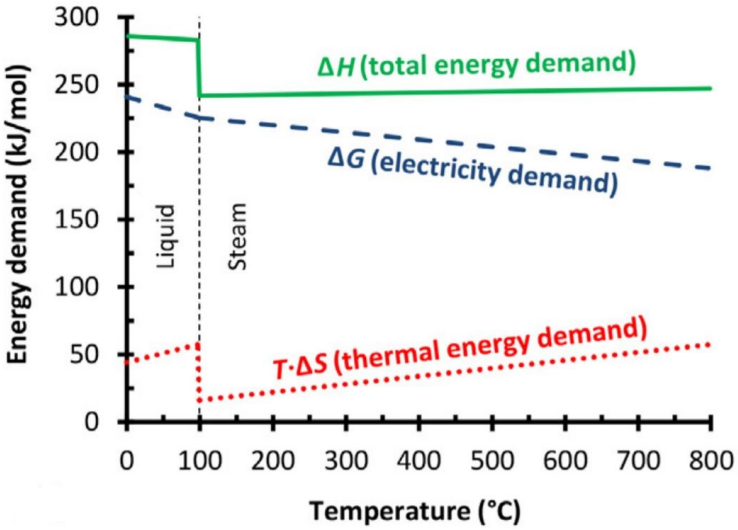

Figure 10: Temperature dependence of main thermodynamic parameters for water electrolysis at 1 bar [50].

To conclude, when the cell voltage is higher than 1.48 V heat is released to the surroundings. A high current also contributes to more heat losses to the surroundings. The higher the heat losses the less efficient the electrochemical cell is. The cell voltage needed is dependent on the characteristics of the electrochemical cell and the current density J. A way to determine the cell voltage is by using a polarisation curve. This will be discussed in chapter 4.

3.3 Heat recovery

Whether the heat released during electrolysis can be recovered depends on the amount and temperature of the released heat. Waste heat can be classified into high temperature, medium temperature and low temperature grades. For the different classes different waste heat recovery systems can be used [51]. High temperature waste heat has a temperature higher than 400 °C, medium temperature waste heat has a temperature between 100-400 °C and low temperature waste heat has a temperature below 100 °C [52]. The higher the temperature of the waste heat, the higher the quality of the waste heat and therefore the bigger the chance the waste heat can be recovered and used. To calculate the amount of available waste heat in J, equation 15 can be used.

$$Q = V \times \rho \times C_p \times \Delta T \tag{15}$$

Q is equal to the heat content in Joule, V is the flowrate of the substance in m^3/s, ρ is the density of the gas in kg/m^3, C_p is the specific heat of the substance in J/kgK and ΔT is the difference in temperature between the outlet and the inlet of the electrolyser stack in K. To determine which heat recovery system can be used it is essential to research the amount and temperature of heat recoverable from the process. There are many different heat recovery systems known, however, some systems seem more promising than others and two are mentioned here briefly.

When making use of direct thermodynamic cycles it is possible to use waste heat to directly produce electrical energy and improve the energy efficiency. One of these thermodynamic cycles that could be used as waste heat recovery system is the organic Rankine cycle (ORC). The ORC uses organic substances with low

boiling points and high vapour pressures as the working fluid to generate power instead of water or steam [53]. An ORC consists of a heat exchanger, evaporator, preheater, generator, condersor, pump, recuperator and a cooling tower. For thermodynamic cycles waste heat of medium to high temperatures is needed [51]. For waste heat of low temperatures an organic Rankine cycle is not considered a beneficial heat recovery system. For low temperature waste heat a heat pump could be of use. A heat pump is a thermodynamic device which takes and transfers heat from a heat source to a heat sink using a small amount of energy [54]. Heat pumps have the capability to upgrade waste heat to a higher temperature and quality, which is useful for waste heat that is of lower temperature [51]. How efficient a heat pump is, is dependent on the ratio between the heat output from the condenser and the power supplied to the compressor. This relation is shown in equation 16.

$$\text{COP} = \frac{Q}{W} \tag{16}$$

Where Q is equal to the heat output in J and W is equal to the work in J. COP is the coefficient of performance. In equation 17 the relationship between the input and the output temperatures is shown.

$$\text{COP}_{\text{heating}} = \frac{T_H}{T_H - T_C} \tag{17}$$

T_H represents the output temperature in K and T_C represents the input temperature in K. $COP_{heating}$ indicates a heating process like a heat pump.

3.4 Existing models and limitations

After extensive research into waste heat recovery from an electrolyser, it has become clear that almost no previous research has been done on the matter. This could indicate that research still needs to be carried out. On the other hand, two projects where found where electrolysers will be built and the waste heat used. One of the projects is called Get H_2 Lingen and is located in Germany. In figure 11 an overview of the project is shown.

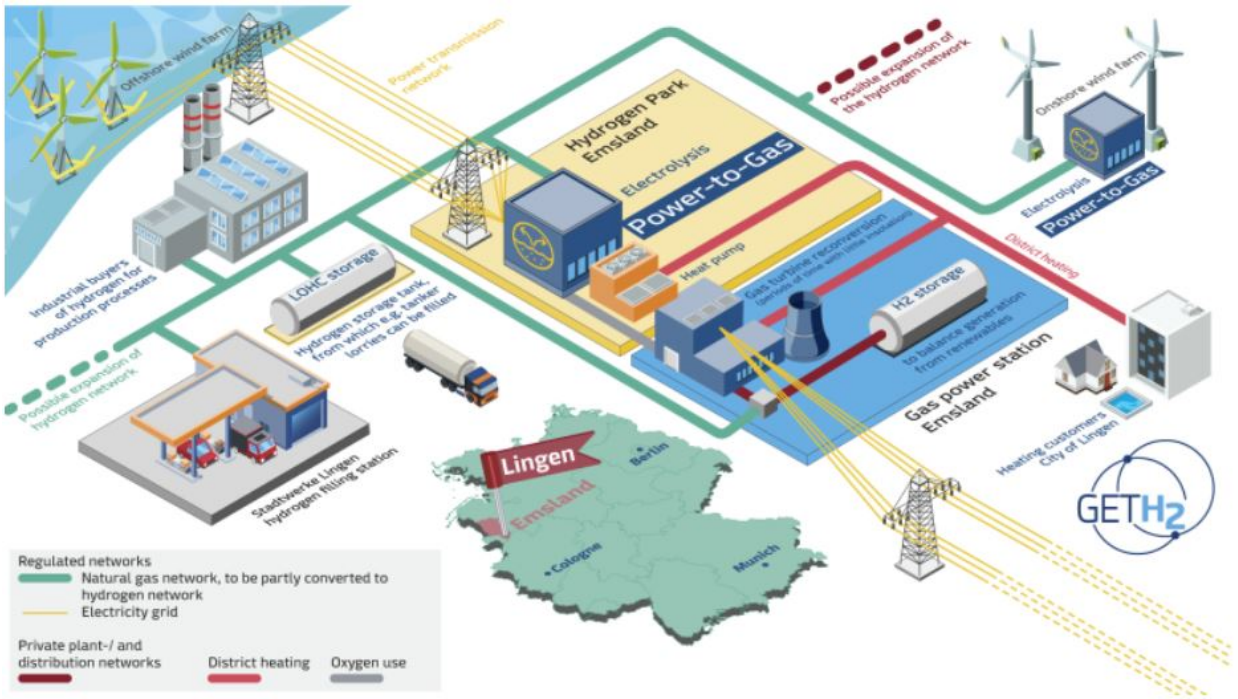

Figure 11: Project Lingen [55].

In the project Get H_2 Lingen a heat pump is implemented for using the waste heat from electrolysis as district heating. More detailed information about this project has not been found. A second project where the waste heat of an electrolyser is going to be used is the GROHW project displayed in figure 12.

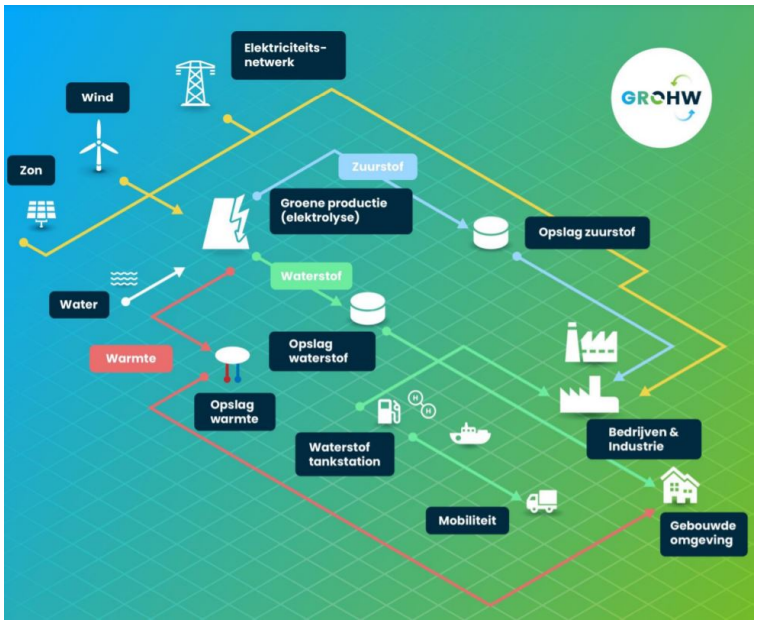

Figure 12: Project GROHW [56].

GROHW stands for Green Oxygen, Hydrogen and Waste heat. In this project a PEM electrolyser will be used. The waste heat will be used for the build environment. Unfortunately, the GROHW project also just started and any in depth details are not known yet. In summary, there is interest for using the waste heat from electrolysis. However, how this goal can be reached is still vague and not detailed yet. Further research needs to be carried out.

This same conclusion was made by ir. W.J. Tiktak in his work. Little research has been done on the excess heat produced by electrolysis, thus Tiktak. Therefore, Tiktak studied the potential of excess heat from medium- to large-scale PEM electrolysis. A model was built in Matlab and Simulink and the conclusion was made that it is possible to contain at least 92 % of the heat produced by the stack of cells. The biggest contributor to the irreversible loss of heat was found to be water vapour in the product flow of the electrolyser. It was concluded that these losses could be minimized by an elevated anode pressure. The contained low temperature heat serves well for applications such as space heating and/or water heating. Research was also done for an offshore scenario. Finding use for the excess heat in an offshore environment proved to be more challenging. There is no direct application available on an island or platform for low temperature heat, apart from preheating the process water. By making use of a heat pump high enough temperatures could be created to aid in thermal desalination. The use of an organic Rankine cycle was also investigated, although this did not have a positive outcome [57].

Much research has been conducted on the topic of using thermal energy from an engine in combination with an electrolyser cell. For example, in the work of Wang et al. the integration of a solid oxide electrolyser with an engine waste heat recovery system, that uses waste heat to heat the water to steam, is researched. It is concluded that utilization of engine waste heat for SOEC increases the electrical efficiency [58]. This leads to the question, will this also be the case when using the waste heat from the SOEC itself? To investigate this, a model should be built. A tool that is used in different research to model an electrolyser is called ASPEN.

4 Method

This chapter is intended to describe the model and methodology used for answering the research questions. To answer the research questions an alkaline water electrolyser is designed in ASPEN.

4.1 ASPEN

ASPEN is a process simulation software package that is widely used in industry [59]. ASPEN's primary use is to aid in the computer simulation of chemical plants that operate at steady state. ASPEN contains a collection of mathematical models for different kinds of chemical process equipment such as heat exchangers, pumps, compressors, turbines, distillation columns, absorbers, strippers and chemical reactors. Some of these mathematical models are simple and could also be calculated by hand, but the power of ASPEN is that it has the ability to link hundreds of models of process equipment into a process system, thus constructing a large model which represents an entire chemical plant containing potentially millions of equations. ASPEN can then run a simulation solving the equations of the model and finding the unknown values of the process [60]. In literature ASPEN is often used to build models and flow diagrams of electrolysers. Therefore, ASPEN can be considered as a tool that can be used for the simulation and models of water electrolysers for the production of hydrogen [61].

4.2 Overview model

An overview of the alkaline electrolyser model build in ASPEN is shown in figure 13. The electrolyser consists out of three elements namely the stack, the anodic circuit and the cathodic circuit. These different elements will be further explained in the following subchapters.

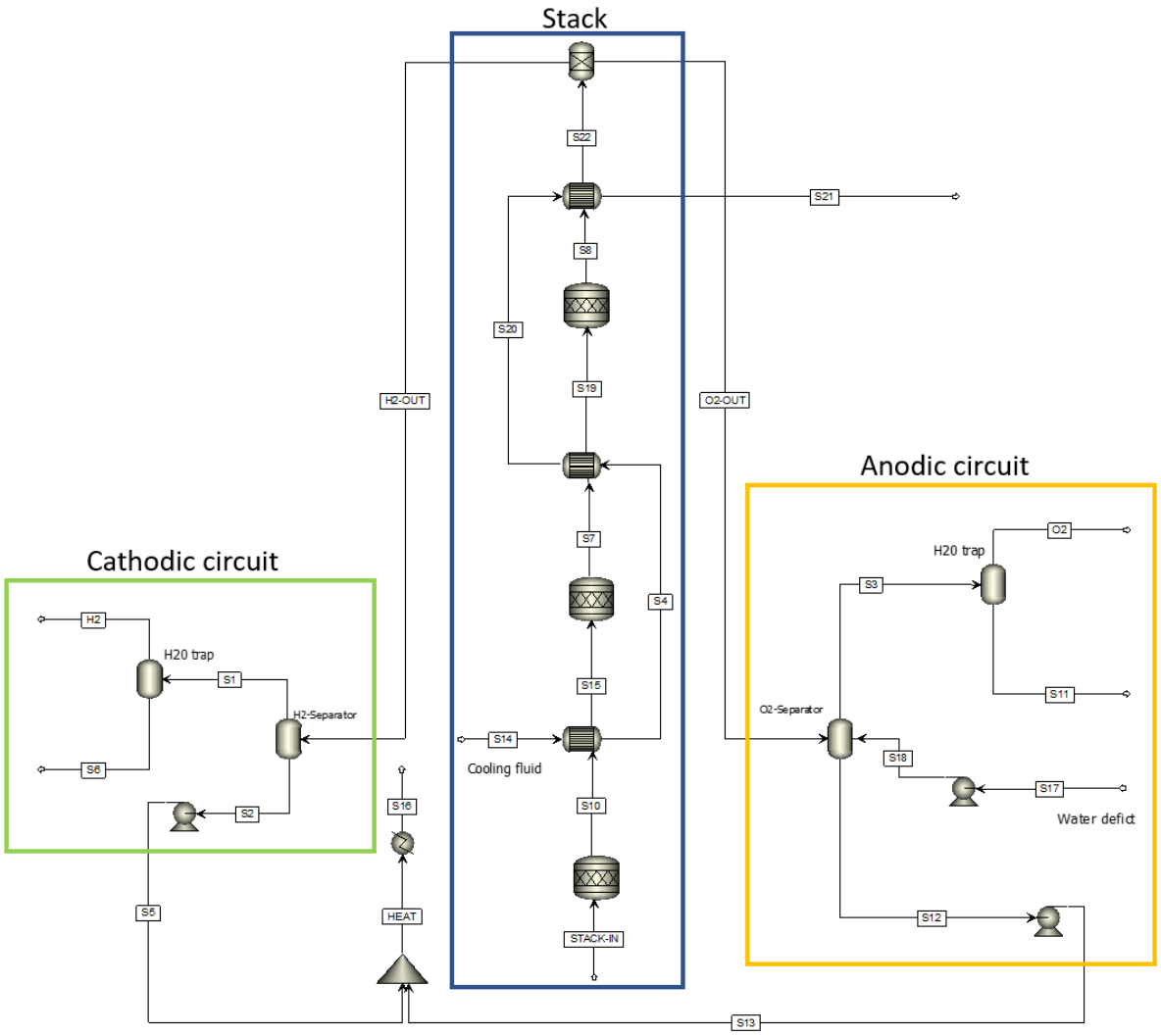

Figure 13: Process model of an alkaline electrolyser in Aspen plus.

To develop the alkaline electrolyser model different submodels and input and outputs are needed. The different input and outputs needed for the electrolyser model are shown in figure 14. The overall alkaline electrolyser model will consist out of three submodels. The first being the electrochemical model. The model simulates the relation between the current and the cell voltage. The thermal model will simulate the generated heat, the heat loss and the amount of heat that needs to be cooled. The cooling system is designed so that the temperature of the stack will be within a desired temperature range.

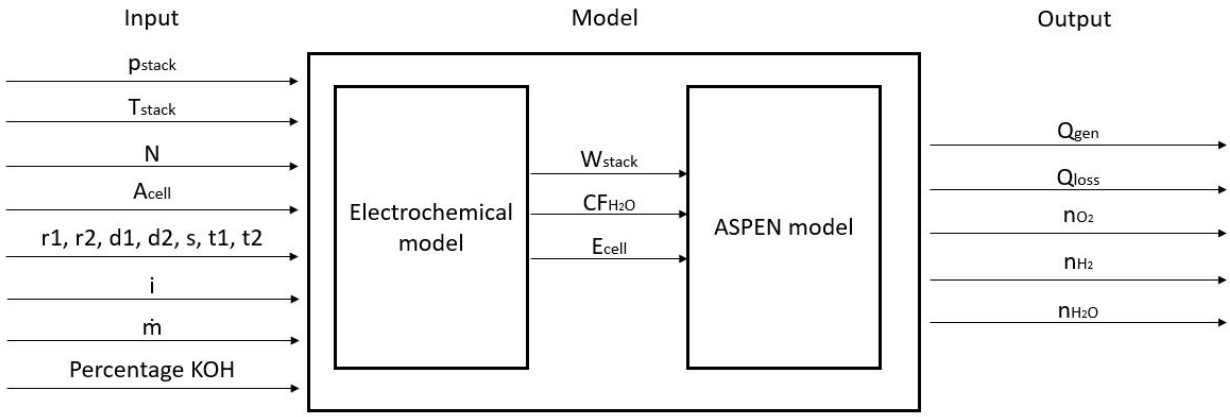

Figure 14: Model input & output.

The input values for the alkaline electrolyser model are based on literature and on a test bench. The test bench, developed by Centro Nacional del Hidrógeno, is used as a reference [61]. Corresponding inputs are shown in table 4.

Table 4: Model inputs.

Coefficient	**Value**	**Unit**
p_{stack}	7.00	bar
T_{stack}	75	°C
N	12	-
A_{cell}	0.1	m^2
KOH fraction	35	%
ṁ	900	kg/s
i	4200	A/m^2
r1	$4.45153*10^{-5}$	Ω m^2
r2	$6.88874*10^{-9}$	Ω m^2 $°C^{-1}$
d1	$3.12996*10^{-6}$	Ω m^2
d2	$4.47137*10^{-7}$	Ω m^2 bar^{-1}
s	0.33824	V
t1	0.01539	m^2 A^{-1}
t2	2.00181	m^2 °C A^{-1}
t3	15.24178	m^2 $°C^2$ A^{-1}

4.2.1 Stack

An electrolyser stack consists of several cells linked in series. These cells can be linked as unipolar or bipolar. In the unipolar design the electrodes are negative or positive with parallel electrical connection of the individual cell. In the bipolar design, the individual cells are linked in series electrically and also geometrically. An example of the different cell designs is shown in figure 15.

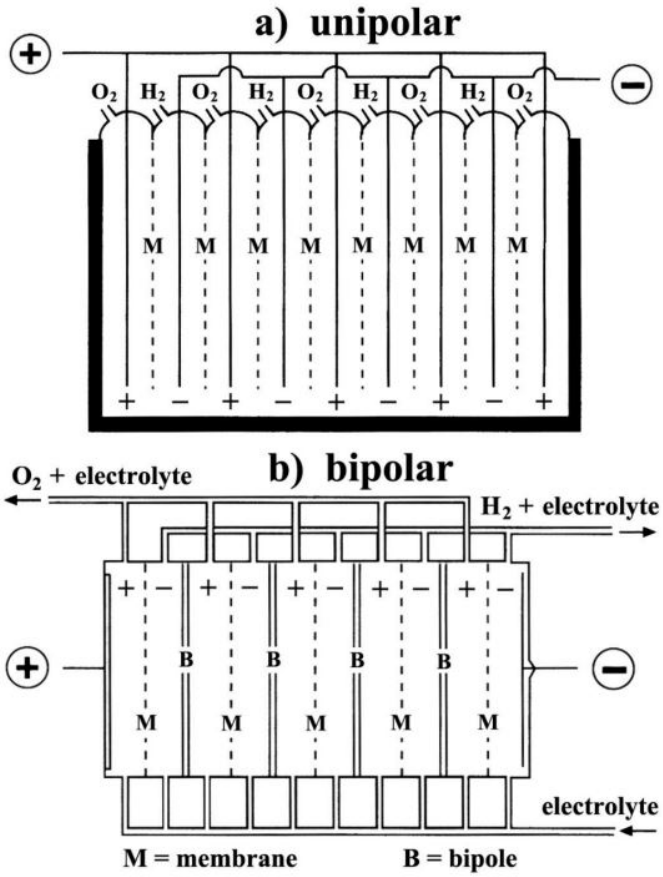

Figure 15: Principle of an a) unipolar electrolyser design b) bipolar electrolyser design [62].

The cells in the stack of the alkaline electrolyser model in ASPEN are linked in a bipolar manner. This choice was made because of two reasons. Firstly, most commercial alkaline electrolysers have cells that are linked bipolar and secondly, as earlier mentioned, a test bench, developed by Centro Nacional del Hidrógeno, is used as a reference. The test bench is composed of a cell stack of 12 bipolar alkaline electrolysis cells. Since Aspen Plus does not include an operation unit for modelling an alkaline electrolysis cell stack, every stack of cells of 12 bipolar alkaline electrolysis cells is modelled as one stoichiometric reactor. Between every stack of cells a heat exchanger is placed, this design will be explained more in depth in chapter 4.5.

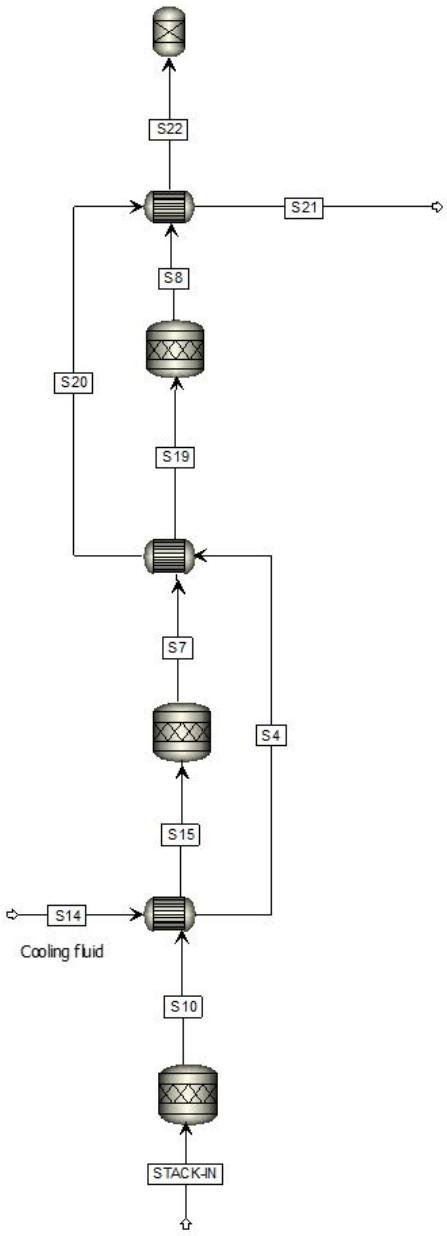

Figure 16: Stack design in ASPEN for the alkaline electrolyser.

The inputs needed for the stoichiometric reactor are the reaction stoichiometry, which is equal to equation 18, the pressure, which is set at 7 bar and the duty. The duty can be calculated with equation 19 [61]. For this equation a value for E_{cell} is needed. The method of determining this value will be explained in more detail in the electrochemical model in chapter 4.3.

$$\mathrm{H_2O} \rightarrow \mathrm{H_2(\ Mixed\ )} + 0.5\ \mathrm{O_2(Mixed)} \tag{18}$$

$$W_{\text{stack}} = E_{\text{stack}} \cdot I = (E_{\text{cell}} \cdot N) \cdot (i \cdot A_{\text{cell}}) \tag{19}$$

After the stack, the produced hydrogen, oxygen and electrolyte are led to a separator. In the separator the hydrogen and oxygen are separated through distillation into two streams as can be seen in figure 17. The product streams go to the anodic and the cathodic circuit.

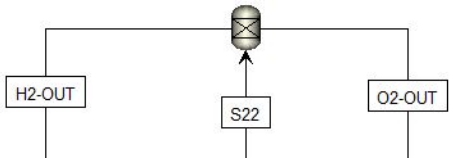

Figure 17: Flash for separating oxygen and hydrogen.

4.2.2 Anodic circuit

At the anode, oxygen is produced as can be seen in equation 5. In the anodic circuit the oxygen is separated from the electrolyte. First, the O_2-out stream is led to a separator where the O_2 is separated from the electrolyte and where new water is inserted to the process. The oxygen stream is then led to a H_2O trap where the oxygen and water is separated a second time to produce more pure components and to lower the temperature of the end products to 25 °C. The water stream will go to a pump where the pressure, in case of pressure losses, will be pumped to 7 bar. For the pumps in the system a pump efficiency of 0.7 was chosen [63]. An overview of the anodic circuit is shown in figure 18.

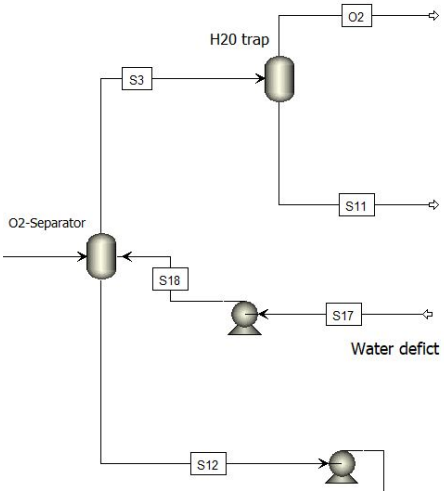

Figure 18: Anodic circuit design in ASPEN for the alkaline electrolyser.

4.2.3 Cathodic circuit

At the cathode, hydrogen is produced as can be seen in equation 6. In the cathodic circuit the hydrogen is separated from the electrolyte. First, the H_2-out stream is led to a separator where the H_2 is separated from the electrolyte. The hydrogen stream is then led to a H_2O trap where the hydrogen and water are separated a second time to produce more pure components and to lower the temperature of the end products to 25 °C. The water stream will go to a pump where the pressure, in case of pressure losses, will be pumped to 7 bar. An overview of the cathodic circuit is shown in figure 19.

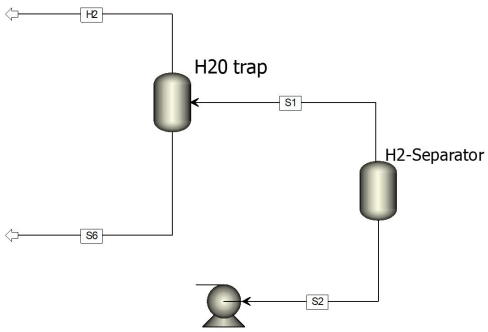

Figure 19: Cathodic circuit design in ASPEN for the alkaline electrolyser.

The hydrogen production rate at the cathode depends on the electrochemical behavior of the cells and can be determined using the Faraday efficiency shown in equation 20. η_{Faradic} can be determined with help of equation 21 [62].

$$n_{\text{H}_2,\text{prod}} = \eta_{\text{F}} \cdot \frac{\text{I}}{\text{z} \cdot \text{F}} \cdot \text{N} \tag{20}$$

$$\eta_{\text{Faradic}} = \Delta\text{G}_{\text{cell}} \,/\, (\Delta\text{G}_{\text{cell}} + \text{losses}) = \text{E}^{\text{o}}/\text{E}_{\text{cell}} \tag{21}$$

4.3 Electrochemical model

The electrochemical model forms the basis for the stack. The electrochemical model is based on the work of Ulleberg [64] and on the work of Sanchez et al. [61]. Ulleberg has developed a mathematical model for an alkaline electrolyser. The model is based on a combination of fundamental thermodynamics, heat transfer theory and empirical electrochemical relationships. The model is widely used and can predict the cell voltage, hydrogen production, efficiencies and operating temperature. Ulleberg makes use of emperical relations for modelling the most complex electrochemical processes, however an attempt is made to make the model as generic as possible and applicable to all different types of alkaline electrolysers [64]. Most of the heat is produced in the stack. The electrochemical model simulates the relation between the waste heat, the current and the cell voltage. The cell voltage of an electrolyser can be determined by equation 22.

$$E_{\text{cell}} = \eta_{\text{ocv}} + \eta_{\text{act}} + \eta_{\text{trans}} + \eta_{\text{ohm}} \tag{22}$$

Where η_{ocv} represents the open circuit voltage, η_{act} represents the activation overpotential, η_{trans} represents the mass transport overpotential and η_{ohm} represents the ohmic and ionic overpotential [42]. The influence and size of these losses can be made insightful with the help of a polarisation curve. In figure 20 a polarisation curve of an alkaline electrolyser is shown.

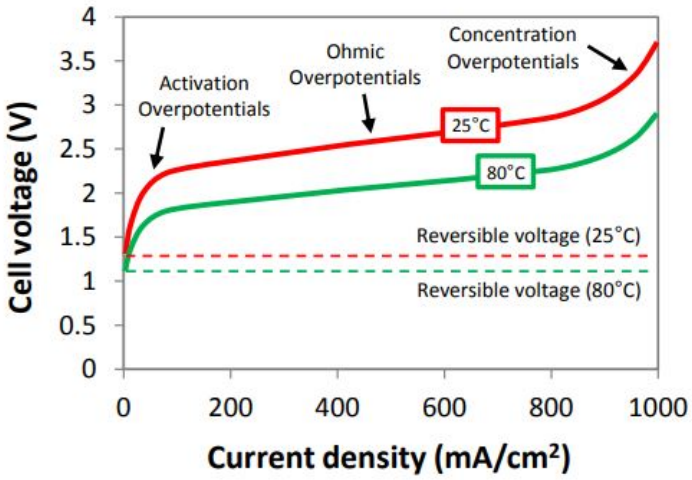

Figure 20: Polarisation curve of an alkaline electrolysis cell at 25 °C and 80 °C [65].

Figure 20 shows that all losses together equal the voltage of the cell, as was stated in equation 22. At lower current densities the activation losses contribute the most. At higher current densities mass transport losses (concentration overpotential) are the biggest contributing factor. Ohmic losses increase linearly with the current density. These losses are due to the resistance for the flow of ions (OH^-) in the electrolyte and the electrical resistance for electrons of the electrodes. An overview of the different losses and the influence on the thermodynamic maximum is shown in figure 21.

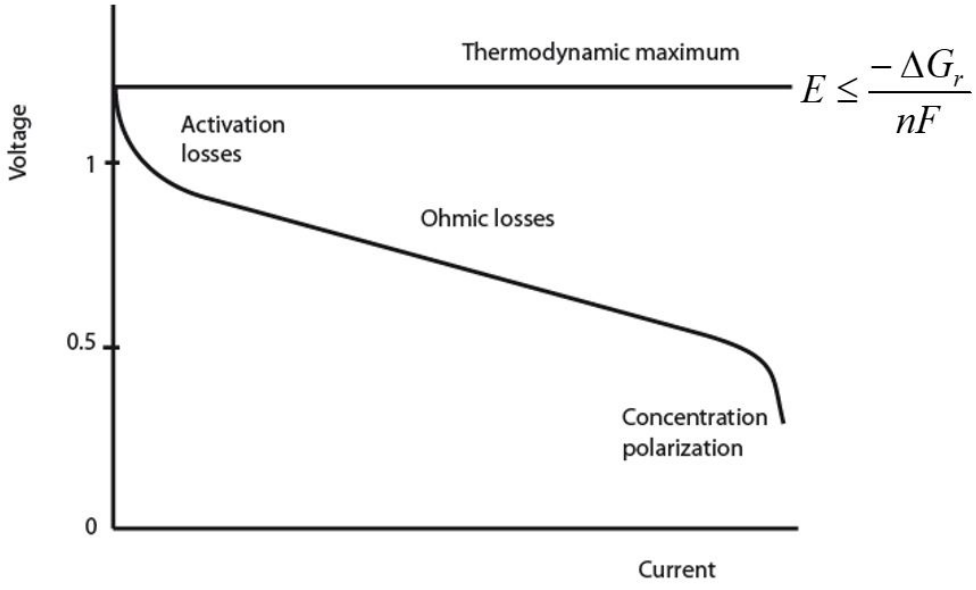

Figure 21: Overview of the influence of losses on the thermodynamic maximum of an electrolyser [42].

According to the model of Ulleberg E_{cell} can also be represented by equation 23.

$$E_{cell} = E_{\text{rev}} + ri + s\log(ti + 1) \tag{23}$$

Where the first term is equal to the reversible cell potential. The second term relates the ohmic overpotentials by r. The last term represents the activation overpotentials, which are defined by the parameters s and t. i is equal to the current density in A/m^2. The coefficients for t and r are described as a function of temperature which can be seen in equation 24 and equation 25.

$$t = t_1 + \frac{t_2}{T} + \frac{t_3}{T^2} \tag{24}$$

$$r = r_1 + r_2 \cdot T \tag{25}$$

The parameter s is assumed a constant value. To make this model also pressure dependent, an additional parameter d has been added. It represents the linear variation in the ohmic overpotentials according to the pressure. An equation for parameter d is shown in equation 26.

$$d = d_1 + d_2 \cdot p \tag{26}$$

By adding the pressure dependent parameter d, equation 23 is expanded to equation 27. The following subchapters will further explain how these coefficients are related to the different overpotentials which are relevant for alkaline electrolysis.

$$E_{cell} = E_{\text{rev}} + ri + di + +s \log\left(ti + 1\right) \tag{27}$$

4.3.1 Open circuit voltage

The open circuit voltage is known as a reversible voltage. It is defined as the potential difference between the cathode and the anode when no reaction is taking place and when the current is zero [66]. When equation 11 and equation 14 are combined, the following reaction can be defined.

$$E_{\text{rev}} = -\frac{\Delta H - T\Delta S}{nF} = -E_{\text{th}} + \frac{T\Delta S}{nF} \tag{28}$$

Where E_{th} is the earlier mentioned thermoneutral potential. The Nernst equation, specified for hydrogen, is shown in equation 29. It gives as output the open circuit voltage or cell potential. This cell potential can be calculated at known standard conditions [49].

$$E = E^0 + \frac{RT}{nF} \ln \frac{a_{O_2}^{1/2} a_{H_2}}{a_{H_2O}} \tag{29}$$

In equation 29 R is the absolute gas constant, equal to 8.314 J/mol/K. E^0 is the standard value of the equilibrium cell in V and T is the absolute temperature in K. $a_{O_2}^{1/2}$, a_{H_2} and a_{H_2O} are the activities of water, oxygen and hydrogen in the electrolyte [45]. The activity of the gasses can also be represented by the effective partial pressure denoted by $p_{O_2}^{1/2}$ and p_{H_2} [67]. Under standard conditions E^0 has the same value as E_{rev}, however the electrochemical model does not operate under standard conditions. E^0 can be calculated with equation 30 and is temperature dependent [29] [68].

$$E^0 = 1.5184 - 1.5421 \times 10^{-3} T + 9.523 \times 10^{-5} T \times \ln T + 9.84 \times 10^{-8} T^2 \tag{30}$$

A value of 75 °C will be used in the electrochemical model as can be seen in table 4. Therefore, the value of E^0 is equal to 1.1875. In the electrochemical model the pressure difference in the stack is not taken into account. The pressure is assumed to be constant. Therefore, at a pressure of 7 bar, E would be equal to 1.188 V + 0.04376 V, which is 1.231 V. Some alkaline electrolysers, like the electrolyser from Alliander, work up to 30 bar. Under those circumstances E would be equal to 1.264 V. In the model of Ulleberg and Sanchez et al. the open circuit voltage is not of importance. For the open circuit voltage the value of E_{rev} of 1.229 V is used.

4.3.2 Activation overpotential

The activation overpotential is an energy loss which is equal to the amount of energy required to start the reaction. This loss is directly affected by the catalyst material, utilisation, temperature and load [42]. The activation overpotential can be determined by the Butler-Volmer equation. The Butler-Volmer equation is used to describe the kinetics of the electrodes [67]. In equation 31 the Butler-Volmer equation is shown.

$$\frac{i}{i_0} = \exp\left(\frac{\alpha_{\text{a}} F \eta_{act}}{RT}\right) - \exp\left(\frac{-\alpha_{\text{c}} F \eta_{act}}{RT}\right) \tag{31}$$

i_0 is the exchange current density in A/m^2. The exchange current density is the magnitude of both the anodic and the cathodic current densities when a working electrode is at an equilibrium potential, such that the anodic and cathodic current densities are equal and opposite and the total current is zero. The magnitude of the exchange current density can vary between 10^{-16} to 10^3 A/cm^2. A high exchange current density indicates a fast reaction and a highly reversible system [6]. α_a and α_c are transfer coefficients for both the anodic and the cathodic current. The coefficients are unitless. In older textbooks a Butler-Volmer equation is found where the transfer coefficients are scaled by the value of n, the number of electrons transferred. According to recent research this is not correct and the transfer coefficients should not be scaled by the value of n. The simultaneous release or uptake of more than one electron is regarded as highly improbable in view of the absolute rate theory of electron transfer of Marcus [69][70]. At values of an overpotential of approximately 10mV, one term of the Butler-Volmer equation is usually more significant than the other. The lower contributing term can be removed from the equation. As a result, the anodic and cathodic Tafel equations are formed which are shown in equation 32 and 33[71].

$$\eta_{act,a} = \frac{RT}{\alpha_a F} \ln\left(\frac{i}{i_{0,a}}\right) \tag{32}$$

$$\eta_{act,c} = -\frac{RT}{\alpha_c F} \ln\left(\frac{i}{i_{0,c}}\right) \tag{33}$$

When $\eta_{act,c} = \frac{RT}{\alpha_a F}$ gives a high value the electrochemical reaction is slow. A high value for i_0 indicates that the reaction is faster than for a low value for i_0 [6].

In the model of Ulleberg and Sanchez et al. equation 34 is used for the activation overpotential. This relation is found by a empirical model and experimental validation and has been broadly accepted. As earlier mentioned, the coefficients for t are described as a function of temperature and the parameter s is assumed to be a constant value. In figure 22 the activation overpotential is shown at different current densities.

$$\eta_{act} = \text{s} \cdot \log\left(\left(t_1 + \frac{t_2}{T} + \frac{t_3}{T^2}\right) \cdot i + 1\right) \tag{34}$$

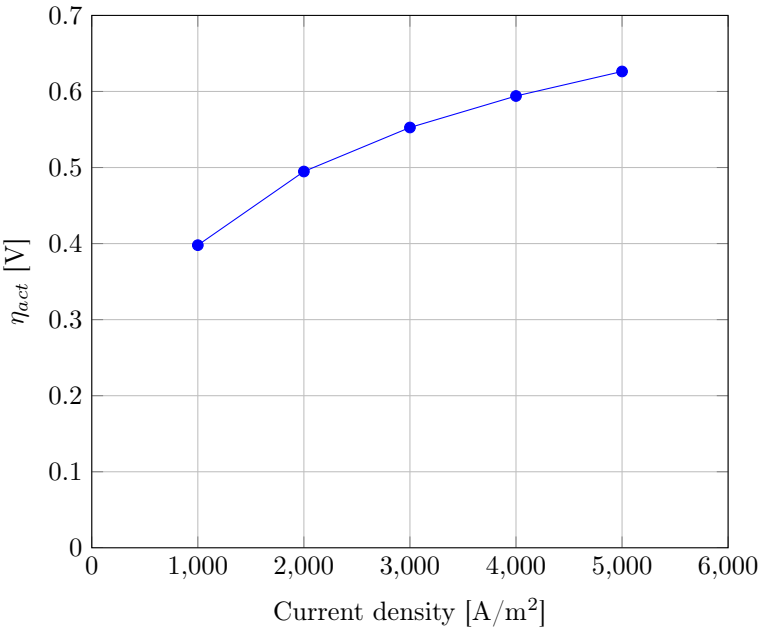

Figure 22: Activation overpotential at 7 bar and 75 °C.

4.3.3 Mass transport overpotential

Mass transfer can occur in electrolysis when the diffusion of products is not fast enough. Mass transfer can also occur when the reactant (water) that reaches the electrode surface is consumed immediately, resulting in insufficient reactant on the electrode surface [72]. The mass transport in the electrodes is driven by the diffusion of reacting species because of the concentration gradient as well as the permeation caused by the pressure gradient. The mass transport overpotential, also known as the concentration overpotential, can be expressed in the general form shown below.

$$\eta_{\text{trans}} = \frac{\text{RT}}{n\ \text{F}} \ln\left[\frac{\text{i}_\text{L}}{\text{i}_\text{L} - \text{i}}\right] \tag{35}$$

In equation 35 i_L is the limiting current density. i_L can be calculated using equation 36.

$$\text{i}_\text{L} = n \cdot \text{F} \cdot \text{k}_\text{m} \cdot \text{C}_\text{bulk} \tag{36}$$

k_m is the mass transfer coefficient and C_{bulk} is the bulk concentration. The mass transfer coefficient can be calculated with equation 37.

$$k_m = \frac{ShL}{D} \tag{37}$$

The mass transfer coefficient is described by means of Sherwood relations. Where D is the mass diffusivity in m^2/s, Sh the Sherwood number and L the characteristic length in m. PEM electrolysers have porous current collectors. The mass flow through the porous current collectors can be approximated with a diffusion phenomenon, for which Fick's law can be used. Fick's law for diffusion in the x-axis direction is shown in equation 38 [42].

$$J = -D\left(\frac{\partial C_i}{\partial x}\right) \tag{38}$$

J is the diffusive flux and is defined by the number of particles that are moving past a given region divided by the area of that region multiplied by the time interval. The unit of J is mol m^{-2} s^{-1}. D is the diffusion coefficient in m^2s. C_i is the concentration of the gradient in mol/m^{-3} [73]. When combining Fick's law with the Nernst equation it shows that the rate of diffusion limits the reaction rate at higher current densities. This is called the diffusion driven approach. The diffusion driven approach can be applied for both the cathode and the anode and is shown in equation 39 and equation 40. Where $C_{i,mem}$ is the concentration of species i at the membrane electrode interface and $C_{i,mem,0}$ is a working condition taken as a reference [42].

$$\eta_{\text{trans,an}} = \frac{RT_{\text{an}}}{n\ \text{F}} \ln \frac{C_{\text{O}_2,\ \text{mem}}}{C_{\text{O}_2\text{mem,0}}} \tag{39}$$

$$\eta_{\text{trans,cat}} = \frac{\text{RT}_{\text{cat}}}{n\ \text{F}} \ln \frac{\text{C}_{\text{H}_2,\text{mem}}}{\text{C}_{\text{H}_2\text{mem,0}}} \tag{40}$$

In alkaline electrolysers, mass transport overpotential is less relevant. Usually an alkaline electrolyser cell operates between 400 and 600 mA/cm^2. This gives a cell voltage value of around 2.0 V. The polarisation curve in figure 20 shows that concentration overpotentials (mass transport overpotentials) only appear at high currents [65]. Therefore, the mass transport overpotential is not taken into account in this study.

4.3.4 Ohmic overpotential

The ohmic overpotential consists of an electronic and an ionic resistance. There are voltage losses due to the resistance for the flow of ions in the electrolyte and the electrical resistance for electrons of the electrodes. The ohmic overpotential is equal to equation 41 [74].

$$\eta_{\text{ohm}} = R \cdot I \tag{41}$$

During electrolysis hydrogen and oxygen gas bubbles are formed. These bubbles are formed on the surface of the cathode and the anode and, when big enough, will detach from the surface. Thus, the electrode surfaces will be covered by gas bubbles. This reduces the contact between the electrolyte and the electrode, which leads to a blockage of the electron transfer. This increases the ohmic loss of the whole system and adds to the electrical resistance [14].

In the model of Ulleberg equation 42 is used for the ohmic overpotential. Where r_1 and r_2 are parameters related to the ohmic resistance of the electrolyte. The model of Ulleberg only looks at temperature as dependent factor. In the work of Sanchez et al. the influence of pressure was also included. With as result equation 43. The parameters d_1 and d_2 represent the linear variation in the ohmic overpotentials as a function of the pressure [61][64].

$$\eta_{ohm} = (r_1 + r_2 T) \cdot i \tag{42}$$

$$\eta_{ohm} = (r_1 + d_1 + r_2 \cdot T + d_2 \cdot p) \cdot i \tag{43}$$

For the electrochemical model the choice was made to use the model of Sanchez et al. and take the influence of pressure into account. The relation between equation 41 and equation 43 is explained by equation 44 and

equation 45.

$$\eta_{\text{ohm}} = R \cdot A \cdot i \tag{44}$$

$$(r_1 + d_1 + r_2 \cdot T + d_2 \cdot p) = R \cdot A \tag{45}$$

r_1 is the measured resistance at standard conditions per square meter in Ωm^2. r_2 is the measured resistance at non standard conditions minus the measured resistance at standard conditions, varying the temperature per square meter in $\Omega m^2/k$. d_1 is the measured resistance at standard conditions per square meter in Ωm^2. d_2 is the measured resistance at non standard conditions minus the measured resistance at standard conditions, varying the pressure per square meter in $\Omega m^2/bar$. The constant terms d_1 and r_1 could be grouped in a single term. In figure 23 the ohmic and ionic overpotentials are shown at different current densities.

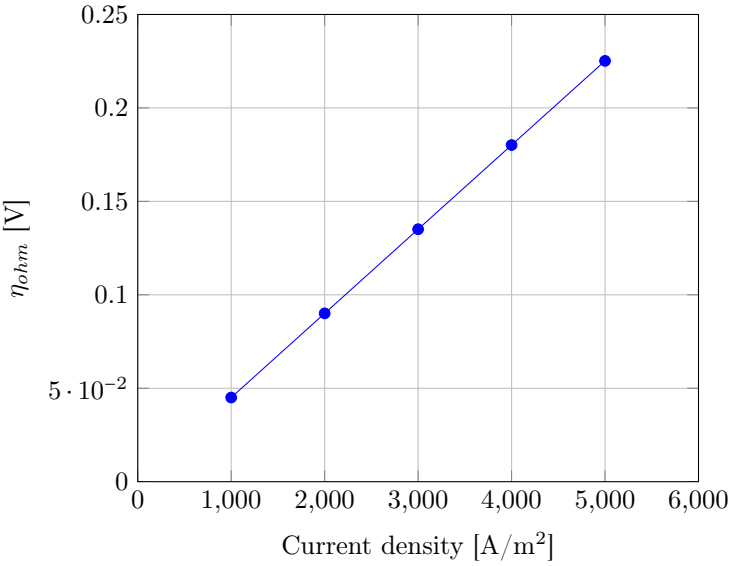

Figure 23: Ohmic overpotential at 7 bar and 75 °C.

4.3.5 Final electrochemical model

To conclude, for an alkaline electrolyser equation 22 can be rewritten to equation 46.

$$E_{\text{cell}} = \eta_{\text{ocv}} + \eta_{\text{act}} + \eta_{\text{ohm}} \tag{46}$$

From this the final model to calculate E_{cell} can be derived, which is shown in equation 47 [75].

$$E_{\text{cell}} = E_{\text{rev}} + [(r_1 + d_1) + r_2 \cdot T + d_2 \cdot p] \cdot i + s \cdot \log\left[\left(t_1 + \frac{t_2}{T} + \frac{t_3}{T^2}\right) \cdot i + 1\right] \tag{47}$$

4.4 Thermal model

The thermal efficiency of the system can be described with equation 48. In an electrolyser, the temperature changes due to heat generation and heat losses. This is shown in equation 49.

$$\eta_{\text{thermal}} = \Delta H_{\text{cell}} \,/\, (\Delta G_{\text{cell}} + \text{losses}) = E_{\text{tn}}/E_{\text{cell}} \tag{48}$$

$$C_t \frac{dT}{dt} = \dot{Q}_{\text{gen}} - \dot{Q}_{\text{loss}} - \dot{Q}_{\text{cool}} \tag{49}$$

Where $C_t \frac{dT}{dt}$ represents the rate of change of the thermal energy of the electrolyser over time. $\dot{Q}_{\text{gen}}$ is equal to the heat generated. The generated heat is created above the thermoneutral potential. $\dot{Q}_{\text{gen}}$ can be calculated with help of equation 50.

$$\dot{Q}_{gen} = N \cdot I \cdot (E_{\text{cell}} - E_{tn}) \tag{50}$$

Due to polarisation, energy losses appear and heat is released during the electrochemical reaction as previously discussed. The heat that is released during electrolysis can be transferred by three different means. Heat conduction, heat convection or heat radiation which are shown in figure 24.

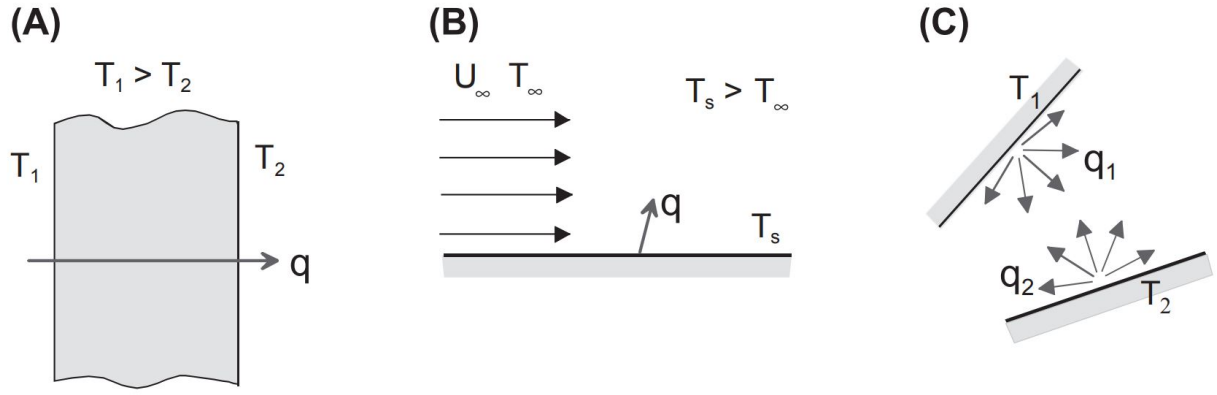

Figure 24: Heat transfer by (A) heat conduction, (B) heat convection and (C) thermal radiation [74].

Heat conduction is the transfer of heat through physical contact. Heat conduction can be calculated by equation 51. Where k represents the thermal conductivity of the medium, A is the cross-sectional area for the heat flow and $\dot{Q}$ represents the heat transfer rate [76][74].

$$\dot{Q} = \frac{kA}{L}(T_1 - T_2) \tag{51}$$

It is possible to replace k/L for U. U is the heat transfer coefficient in W/K m^2. $1/U$ is equal to R. R is the thermal resistivity. This is a useful term when a solid consists of different layers of materials. Heat convection is the transfer of heat from a surface to a fluid. The formula for heat convection is shown in equation 52.

$$\dot{\text{Q}} = hA(T_s - T_f) \tag{52}$$

T_s is equal to the surface temperature and T_f is the fluid temperature. In convective heat transfer a heat transfer coefficient h is used in W/(m^2 K). $1/h$ is equal to the thermal resistivity of convection. A is the surface area in m^2 where fluid and surface are in contact [76]. Thermal radiation is the transfer of heat in the form of electromagnetic waves. It does not require a medium for the propagation and can transfer through vacuum. Thermal radiation can be of influence in SOEC where operating temperatures lie between 800-1200 K. Thermal radiation in electrolysis occurs between the electrodes, when surface to surface heat

exchange takes place. A second form of thermal radiation in electrolysis corresponds to the heat losses from stack to the environment [77]. The formula for thermal radiation is shown in equation 53.

$$\dot{Q} = \varepsilon \sigma A \left(T_2^4 - T_1^4\right) \tag{53}$$

ε is the emissivity of the surface, σ is the Stefan-Boltzmann constant which is equal to 5.669×10^{-8} $\mathrm{W/m^2 \cdot K^4}$ [78]. Equation 53 is used for black bodies. The total emissive power of the surface, denoted by E_b can be calculated using the Stefan-Boltzmann law shown in equation 54.

$$E_b = \sigma T^4 \tag{54}$$

$\dot{Q}_{\mathrm{loss}}$ can be calculated by equation 55. $\dot{Q}_{\mathrm{loss}}$ represents the heat that is lost to the ambient environment. This heat is mostly lost in the form of radiation and convection as can be seen in equation 56 [79].

$$\dot{Q}_{\mathrm{loss}} = \frac{1}{R_{\mathrm{t}}} \left(T_{stack} - T_{\mathrm{amb}}\right) \tag{55}$$

$$\dot{Q}_{\mathrm{loss}} = \sigma \mathrm{A}_{\mathrm{stack}} \, \varepsilon \left(\mathrm{T}_{\mathrm{stack}}^4 - \mathrm{T}_{\mathrm{amb}}^4 \right) + h \, \mathrm{A}_{\mathrm{stack}} \left(\mathrm{T}_{\mathrm{stack}} - \mathrm{T}_{\mathrm{amb}} \right) \tag{56}$$

Heat that gets released during alkaline electrolysis needs to be cooled. The system is modelled in steady state. In steady state equation 49 changes to equation 57. The required amount of cooling is calculated with equation 58. Where cw stands for cooling water.

$$\dot{Q}_{\mathrm{gen}} = \dot{Q}_{\mathrm{loss}} + \dot{Q}_{\mathrm{cool}} \tag{57}$$

$$\dot{Q}_{\mathrm{cool}} = \dot{m}_{\mathrm{cw}} C_{\mathrm{p_{cw}}} \left(\mathrm{T}_{\mathrm{cw,out}} - \mathrm{T}_{\mathrm{cw,in}} \right) \tag{58}$$

4.5 Cooling system

The stack of an alkaline electrolyser needs to be cooled to keep the temperature constant to ensure optimal operation. In commercial alkaline electrolysers the stack is cooled by flowing water, air or the flowing electrolyte. For a small scale alkaline electrolyser a fan or flowing electrolyte could be enough to regulate the temperature of the stack. For larger scale alkaline electrolysers cooling water or air is used that flows through the cells. These current methods are used to get rid of the heat. This heat is then released to the environment. The purpose of the designed cooling system is to recover the heat instead of releasing it to the environment. To achieve this, heat exchangers have been modelled in Aspen. Between every stack of cells a heat exchanger is located. The cooling fluid goes from heat exchanger to heat exchanger. The flowrate of the cooling fluid is set at a value where the cooling fluid, when getting out of the overall stack, is at a temperature between 70 °C and 75 °C. At this temperature the heat could be used in a heat network. In the model water is used as cooling fluid. Water is chosen as cooling fluid because of its high heat capacity and thermal conductivity. Moreover, water is inexpensive and readily available. The temperature of the cooling fluid is equal to 15 °C and at a pressure of 1 bar.

To model the heat exchanger, the program ASPEN exchanger design and rating (EDR) is used. This program helps to find the optimal design for a heat exchanger. To validate if the design, found by ASPEN

EDR, is correct, a plate heat exchanger is added to the model in ASPEN and the following model is made for comparison. The plate heat exchanger makes use of a counter current flow.

Table 5: Conditions of the flows.

Variable	**Fluid 1 (stack)**	**Fluid 2 (water)**
Temperature in T_{in} [K]	From model	288.15
Temperature out T_{out} [K]	348.15	-
Quality X_{in} [-]	1	-
Quality X_{out} [-]	0	-
Mass flow $\dot{m}$ [kg/s]	0.25	Variable
Pressure p [bar]	7	1

The enthalpies of the incoming and outgoing streams according to ASPEN are equal to the following:

$h_{1,in}$= - 13.09 MJ/kg

$h_{1,out}$= - 13.10 MJ/kg

$$\dot{Q}_1 = \dot{m}_{\text{stack}} \ (h_{1,\text{ out}} - h_{1,in}) \tag{59}$$

This results in a value for $\dot{Q}_1$ of - 2.65 kW. When assuming that no heat is lost and all heat is exchanged -$\dot{Q}_1 = \dot{Q}_2$ resulting in $\dot{Q}_2 = 2.65$ kW. With equation 60 $T_{2,out}$ can be calculated. The specific heat capacity $c_{p,2}$ is equal to 4.19 kJ/(kgK) at 15 °C.

$$\dot{Q}_2 = \dot{m}_{\text{water}} \ c_{p,2} \ (T_{2,\text{ out}} - T_{2,\text{ in}}) \tag{60}$$

For a mass flow of 150 kg/h for water, $T_{2,out}$ is equal to 30.2 °C. This is equal to the value in ASPEN. So far the ASPEN heat exchanger is validated. To determine the optimal size of the plate heat exchanger the required surface area for the heat transfer needs to be calculated. The required surface area can be calculated with equation 61.

$$A_0 = \frac{Q_2}{U_{0ass} T_m} \tag{61}$$

Where A_0 is the required surface area. In this formula the duty is represented by Q_2. First, the corrected mean temperature difference, T_m, needs to be determined. To determine the corrected mean temperature difference, the log mean temperature difference, ΔT_{lm}, needs to be determined first. ΔT_{lm} can be calculated with equation 62.

$$\Delta T_{\text{lm}} = \frac{(T_{1,\text{ in}} - T_{2,\text{ out}}) - (T_{1,\text{ out}} - T_{2,\text{ in}})}{\ln \frac{(T_{1,\text{ in}} - T_{2,\text{ out}})}{(T_{1,\text{ out}} - T_{2,\text{ in}})}} \tag{62}$$

Equation 62 gives a value of 53.94 °C for ΔT_{lm}. In order to determine the log mean temperature difference correction factor F_t, it is usually convenient for a plate heat exchanger to first determine the number of transfer units NTU and subsequently the correction factor can be determined using a graph relating these two variables. The number of transfer units is defined as follows:

$$NTU = \frac{T_{2,out} - T_{2,in}}{\Delta T_{lm}} \tag{63}$$

This gives a value of 0.282 for the NTU. According to Sinnott and Towler [80] the correction factor can be determined from the NTU as shown in figure 25.

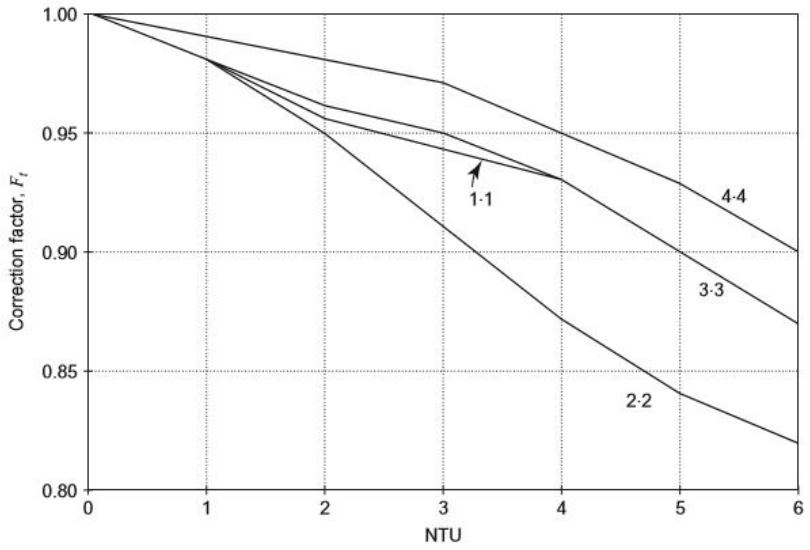

Figure 25: Correction factor F_t as a function of NTU (from Sinnott and Towler [80]).

This gives a value of 0.99 for F_t. With this, the corrected mean temperature can be calculated as shown in equation 64. This gives a value of 53.40 °C for T_m.

$$T_m = F_t * T_{lm} \tag{64}$$

To calculate the required surface area, the estimated overall heat-transfer coefficient, U_{0ass}, also needs to be determined. This can be estimated from literature. A value of 6250 W/m^{2}K is chosen [80]. The required surface area can now be calculated. According to equation 61 A_0 is equal to 7.94*10^{-3} m^2. With these equations the output from ASPEN EDR can be validated. The validation is carried out in chapter 5.3.

5 Results and implementation

This chapter is intended to validate, present and discuss the results of the model developed in ASPEN. The cooling system design, developed in chapter 4.5 will be validated and different heat recovery systems will be discussed. The amount of heat recovered is presented and different possibilities for using the recovered heat are examined.

5.1 Model validation

First, to validate if the model is correct and whether it is a realistic representation of an alkaline electrolyser the output of the model has been compared with findings in literature. In figure 26 an overview is shown of the hydrogen production output of the model and the influence of varying the amount of stacks and with that the overall power of the model.

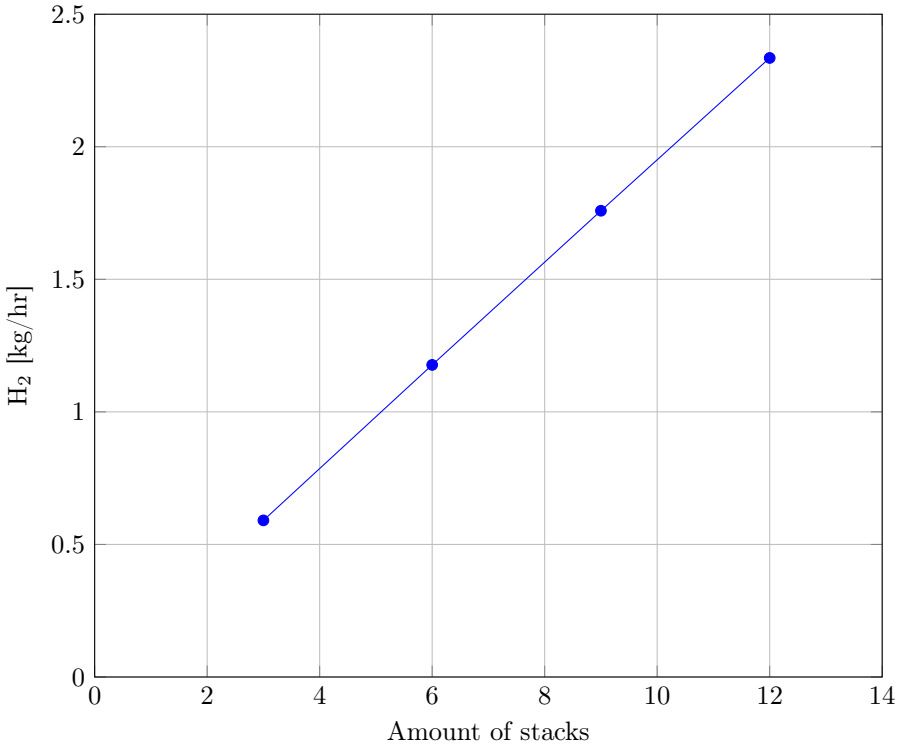

Figure 26: Produced hydrogen at 7 bar and 75 °C.

The relation between the amount of stacks and the amount of hydrogen produced is linear, as shown in figure 26. To validate if the amount of produced hydrogen is realistic and indeed linear, these results are compared to an alkaline electrolyser of the company Nel Hydrogen. Nel Hydrogen specialises in developing electrolysers. The A150 alkaline electrolyser of Nel Hydrogen has a power consumption at the stack of 3.8 to 4.4 kWh/Nm^3 and a net production rate of 50 to 150 Nm^3/h. The A2000 model of Nel Hydrogen has also a power consumption at the stack of 3.8 to 4.4 kWh/Nm^3, however it has a net production rate of 15,520 to 19,400 Nm^3/h [81]. In conclusion, the power consumption at the stack is not dependent on the net production rate and, therefore, the linear relation shown in figure 26 is correct. To validate if the values for the produced hydrogen are realistic, the output of the ASPEN model, consisting out of 12 stacks, is compared

to the production output of the Nel electrolyser. The power consumption at the stack is equal to 122.12 kW. When dividing this number by a mean power consumption at the stack of 4.1 kWh/Nm^3 it results in the production of 29.79 Nm^3/h which is equal to 2.65 kg/h hydrogen. When comparing this output to the output of the ASPEN model a difference of 13.49 % is found. Nel Hydrogen is leading the alkaline electrolyser market and has done much research to develop a reliable and efficient alkaline electrolyser. Therefore, a difference of 13.49 % is not surprising and assumed a realistic value.

The output H_2 stream consists of hydrogen and water. As previously mentioned, hydrogen obtained by electrolysis has a high purity that can reach 99.999 vol.%. A purity of 99.0 vol.% is a minimum for high quality hydrogen. The volume flow and volume fractions of the H_2 output stream are shown in table 6. The ASPEN model produces hydrogen of a purity of 99.84 vol.% and therefore, meets the quality requirements.

Table 6: Volume flow H_2 output stream.

Variable	**Value**
Volume flow [m^3/hr]	1.048
Volume fraction H_2 [-]	0.9984
Volume fraction H_2O [-]	0.0016

5.2 System efficiency

The voltage efficiency, also called thermoneutral efficiency, of an alkaline electrolyser is, on average, between 62-82 %. The voltage efficiency, calculated with help of equation 48, is equal to 73.3 %.

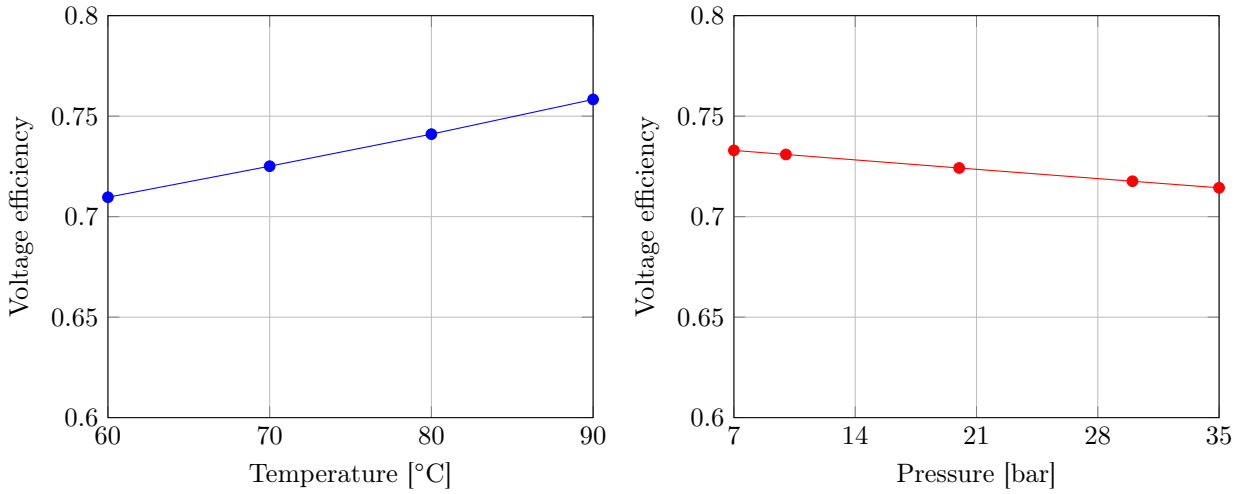

Figure 27: Voltage efficiency as a function of variating temperature and pressure.

The electrical efficiency of the stack can be calculated by equation 65.

$$\eta_{stack} = \frac{n_{\mathrm{H2,OUT}} \cdot \mathrm{HHV_{H2}}}{\mathrm{Duty_{cells}}} \tag{65}$$

HHV_{H2} is the higher heating value of hydrogen and is equal to 285.8 kJ/mol. The duty of the cells is equal to the duty of all the stacks together. The duty needed for cooling is not taken into account for this efficiency. A value of 73.0 % is found for η_{stack}. The overall system efficiency is calculated with help of equation 66.

$$\eta_{system} = \frac{n_{\mathrm{H2,OUT}} \cdot \mathrm{HHV_{H2}}}{\mathrm{Duty_{system}}} \tag{66}$$

$Duty_{system}$ is equal to all duty and work that is put into the system. η_{system} is equal to an efficiency of 72.98 %.

5.3 Cooling system

The optimal design of the plate heat exchanger, designed by ASPEN EDR, is shown in figure 28.

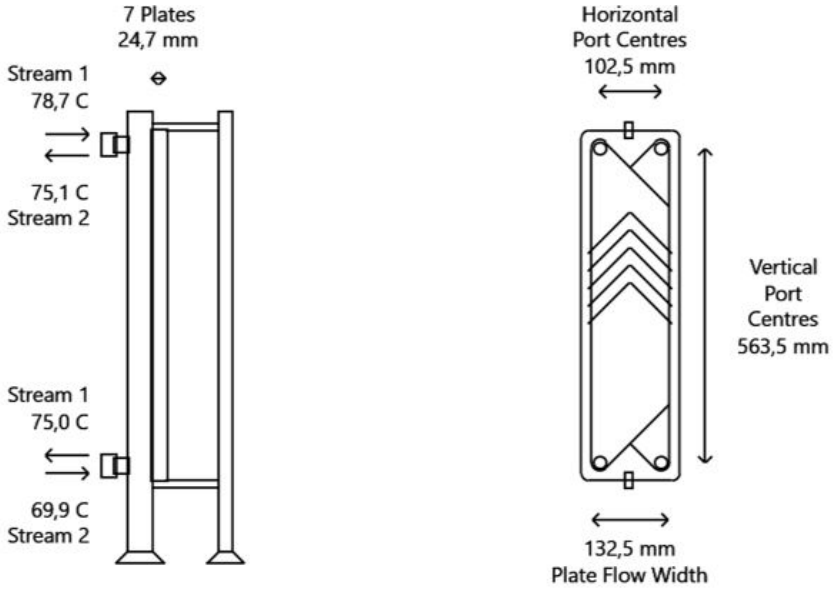

		Plate thickness	0,6 mm
Effective surface area	0,373 m2	Compressed plate pitch	4,1 mm
Number of passes Stream 1 / 2	1 / 1	Area of each plate	0,075 m2
Effective channels Stream 1 / 2	3 / 3	Chevron angle (to horizontal)	45
Number of exchangers	1	Material type	SS-304
		Port diameter	25,0 mm

Figure 28: ASPEN model output plate heat exchanger.

The required surface area, according to ASPEN EDR, is equal to 0.0129 m^2. This value deviates from the $7.94*10^{-3}$ m^2 calculated in chapter 4. The estimation of the overall heat-transfer coefficient, U_{0ass}, appears incorrect. A value of 6250 W/m^2K was estimated, while ASPEN uses a value of 3454.7 W/m^2K. Recalculation of the model resulted in a value of 0.0143 which is in line with the model presented in chapter 4. The ASPEN EDR design for the plate heat exchanger is therefore validated.

The demand for cooling, of the alkaline electrolyser, is shown in figure 29. Considering that the model operates at 75 °C the maximum output of the plate heat exchanger water output stream is as well equal to 75 °C. Therefore, when more heat is produced, a larger cooling fluid stream is needed. This relation is shown in figure 29.

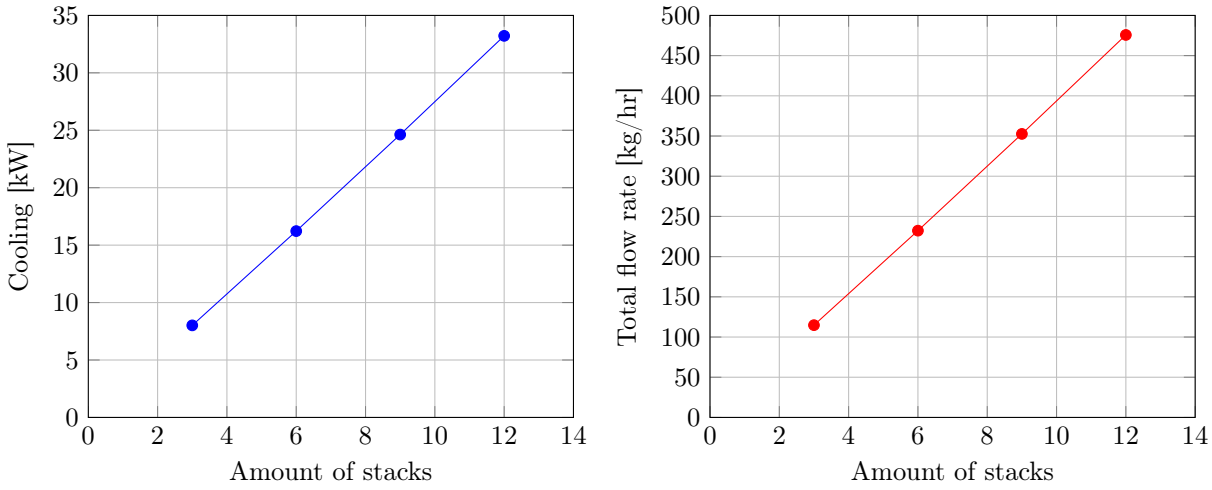

Figure 29: Cooling demand for model operation at 75 °C and 7 bar.

As expected, the amount of cooling is almost linear in relation with the power. As a result the same applies for the total flow rate. The total flow rate can be calculated with equation 67.

$$\dot{m}_{\text{water}} = \frac{\dot{Q}_{\text{total}}}{c_p \left(T_{2,out} - T_{2,in}\right)} \tag{67}$$

According to equation 50 the generated heat is equal to 2717.53 W per reactor. ASPEN gives a value of 2650.0 W for $\dot{Q}_{cool}$. Therefore it can be concluded that for a steady state model $\dot{Q}_{loss}$ is equal to 63.53 W. Therefore the theoretical thermal efficiency when using all the heat that is cooled is equal to 99.4 %. Whether it is possible to achieve this efficiency will be discussed in following subchapters.

5.4 Heat recovery system

To validate the design found by ASPEN EDR, a plate heat exchanger was chosen for recovering the waste heat produced in the stack. However, there are different types of heat exchangers available on the market. To determine which heat exchanger provides the best results for recovering the heat, three different types of heat exchangers are further investigated. The different heat recovery systems are implemented in the ASPEN model and the results and differences will be discussed. The three most commonly used heat exchangers are the shell-and-tube heat exchanger, the plate heat exchanger and the air heat exchanger. In figure 30 the different heat exchanger (HEX) designs are shown.

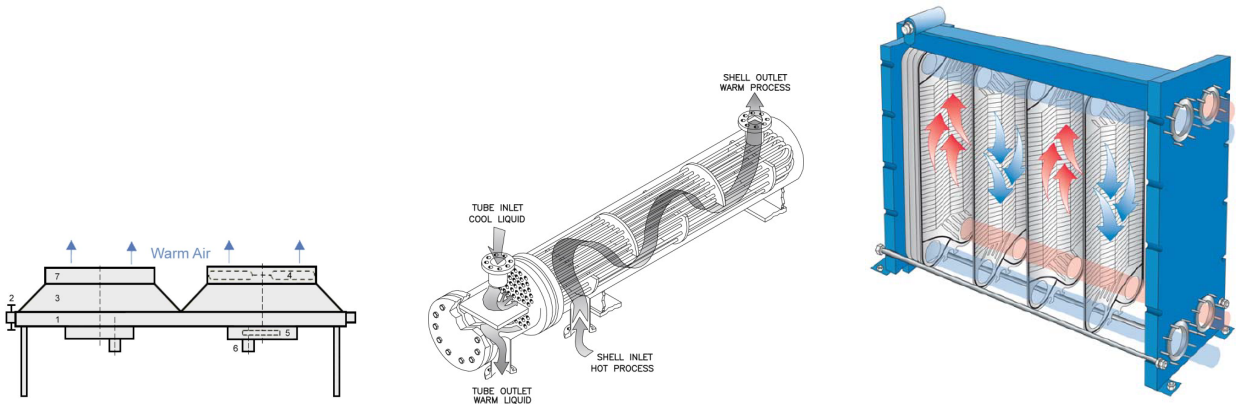

(a) (b) (c)

Figure 30: (a) Forced air HEX [82] (b) Shell & tube HEX [83] (c) Plate HEX [84].

Currrently, in most alkaline electrolysers, an air cooled heat exchanger is used to cool the cells. The air heat exchanger uses air as cooling fluid. Air has a low thermal conductivity and a low heat capacity. Therefore, to cool with air, large equipment is needed which is not favourable. An air cooled heat exchanger requires a large area of a site [85]. The main advantage of the air cooled heat exchanger is that the exchanger uses air instead of water. The main disadvantages are high manufacturing costs, noise and size. According to literature, the main advantages of a shell & tube heat exchanger are a long service life, the possibility of power regulation and internal reliability. Power regulation can be achieved by adjusting the number of sections and the length and diameter of the pipes. Internal reliability implies that cleaning is needed less often than for other heat exchangers. The main disadvantages are the large dimension, low efficiency and vulnerability of the outer part of the case. The main advantages of a plate heat exchanger are the high efficiency, compactness, flexible thermal sizing and the cost. The efficiency of a plate heat exchanger can reach up to 95 %. Next to that, plate heat exchangers are easy to clean. A disadvantage is the short service life, which is up to three years when the installation is not being cleaned. This is due to clogging and regularly cleaning is important [86]. To determine which heat exchanger is the best to use for an alkaline electrolyser, these three different designs have been implemented in the ASPEN model and the results of the model, for the different heat exchangers, are shown in table 7. The design of the different heat exchangers is shown in appendix B.

Table 7: Heat exchangers implemented in the ASPEN model.

Variable	**Plate**	**Shell & tube**	**Shell & tube**	**Air cooled**
Fluid	Water	Water	Air	Air
Flowrate [kg/h]	476	476	1985	1985
Length [m]	0.463	1.829	1.829	2.600
Width [m]	0.133	0.387	0.387	1.020
Cost [$]	761	8768	8768	10322

The plate heat exchanger is the cheapest and smallest heat exchanger and therefore the best choice for recovering the waste heat. The air cooled heat exchanger is the most expensive and the largest heat exchanger. This raises the question, why do most alkaline electrolysers use an air cooled heat exchanger?

In the Netherlands laws exist for releasing cooling water. According to the Activities Decree, cooling water may be discharged into surface water if the heat load does not exceed:

- 1 MW in designated surface waters
- 0.01 MW in non-designated waters (vulnerable)

In which surface waters cooling water may be discharged is determined by the Dutch government and is specified in [87] on pages 746 till 807. In figure 31 one of the regions, de Stichtse Rijnlanden, is shown, as example, with the designated surface water areas shown in (a) and the non-designated surface water areas shown in (b).

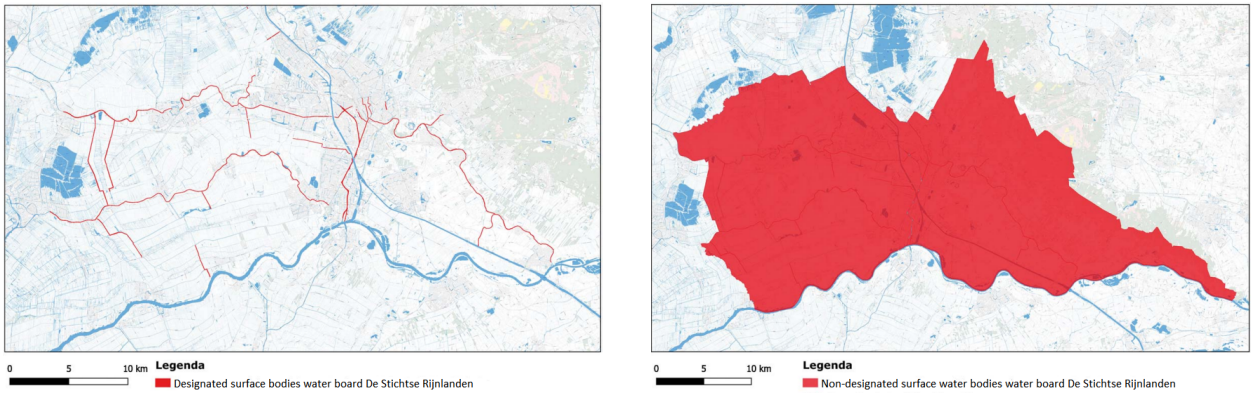

(a) (b)

Figure 31: (a) Designated surface water bodies (b) Non-designated surface water bodies [87].

Figure 31 shows that the designated surface water bodies are scarce. Therefore, the choice to use an air cooled heat exchanger in an alkaline electrolyser makes more sense when the waste heat is not used. Considering that this research is focused on using the waste heat, the plate heat exchanger is the best options for recovering the waste heat.

5.5 Heat recovered

The amount of heat that can be recovered from the alkaline electrolyser stack, developed in ASPEN, is shown in figure 32. As validated in chapter 5.3, the relation between the power and the heat released is almost linear. Therefore, it is possible to predict the amount of heat released when using a bigger installation. The output is shown in figure 33.

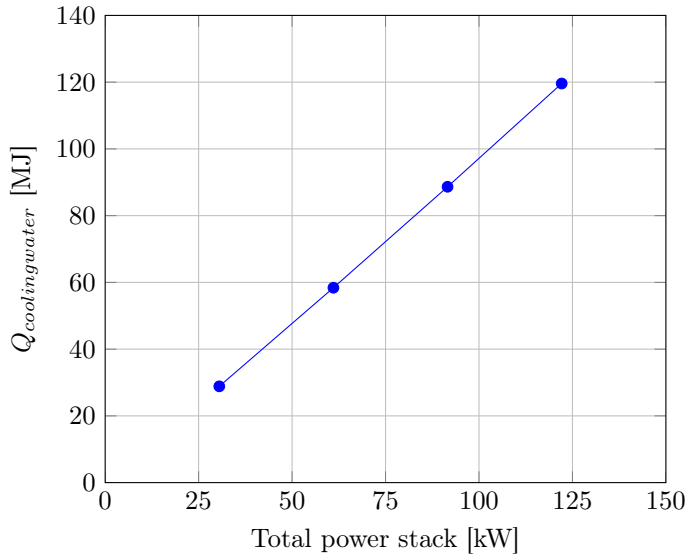

Figure 32: Energy cooling water stream per hour at system operation of 75 °C and 7 bar.

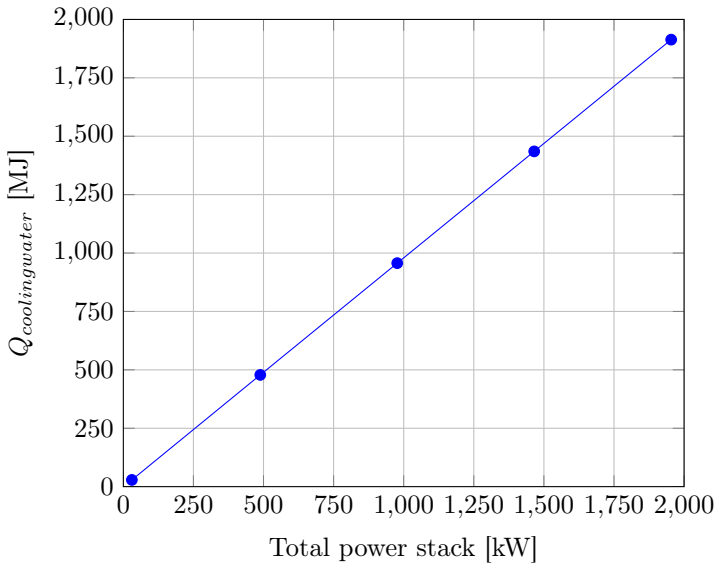

Figure 33: Energy cooling water stream per hour predicted at system operation of 75 °C and 7 bar.

5.6 Heat usage

If the heat, released during electrolysis, can be used is dependent on the location of the electrolyser and dependent on the cooling fluid. Heat can be transported by a heat network. In table 8 an overview of different low temperature heat networks is shown.

Table 8: Low temperature heating [88].

Type of heat network	**Supply temperature**	**Characteristics**
High temperature heat network (HT-network)	>75°C	Direct supply of high-temperature heat for both space heating and hot tap water
Medium temperature heat network (MT-network)	55-75°C	Direct supply of medium-temperature heat for both space heating and hot tap water
Low temperature heat network (LT-network)	30-55°C	Direct supply of low-temperature heat for space heating. Reasonable insulation and LT delivery system needed; domestic hot water by means of a booster heat pump.
Ultra low temperature heat network (ULT-network)	10-30°C	No direct heat supply; very low-temperature heat for a combi heat pump that produces heat for space heating as well as for hot tap water. Reasonable insulation and LT delivery system required.

The heat from an alkaline electrolyser could be transported through the medium temperature heat network. This heat can then be used for space heating and hot tap water. Whether this is possible depends on the location of the electrolyser and the location of the heat network. To minimize losses a heat network needs to be close by. This is important as convection results in heat getting lost. This is described in equation 52. As mentioned before, A is equal to the surface area in m^2 where fluid and surface are in contact. Therefore, the longer the distance, the higher the losses. How high these losses are, is dependent on the type of pipe used and on the isolation used. Practice shows that heat networks have losses of around 20-30 % on an annual basis [88]. In figure 34 an overview is shown of all the medium temperature heat networks in the Netherlands.

Figure 34: Medium heat network projects in the Netherlands [89].

There are several locations where a connection to a heat network is possible. However, using the heat from the alkaline electrolyser model is not an option when the electrolyser is located offshore. Assuming the location of an alkaline electrolyser is onshore, then there is a possibility to connect the alkaline electrolyser to a heat network. The amount of households can be calculated for which the heat can be used. Transport losses of 25 % are assumed. The average consumption of hot water per household equals around 50 m^3 per year. This is equal to around 10 GJ [90]. For what amount of households the heat can be used is shown in figure 35. The output is shown with varying load. An electrolyser works on renewable energy and therefore, the electricity input is not steady. Assuming that the alkaline electrolyser will not work 100 % of the time, the number of households, for which the heat is available, is dependent on the load.

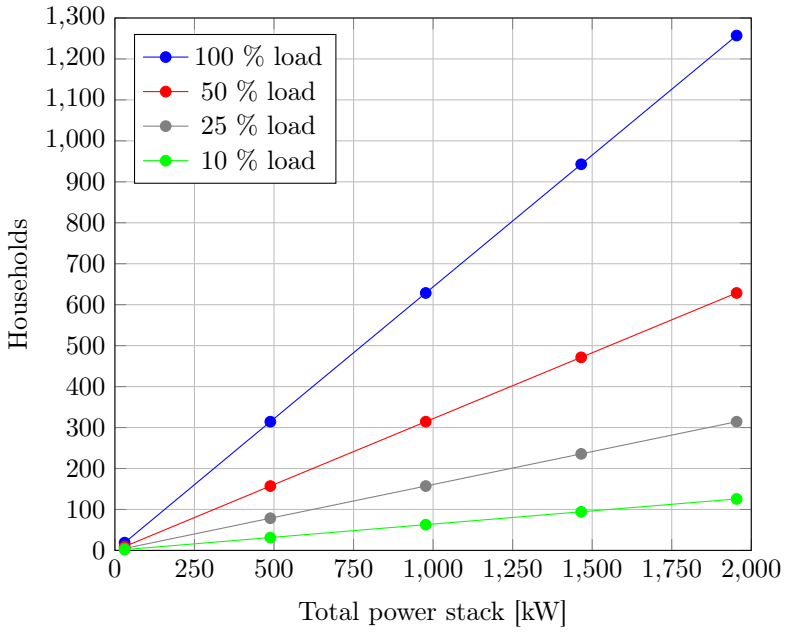

Figure 35: Heat for households considering 25 % losses for transportation.

When assuming transport losses of 25 % and assuming the use of plate heat exchangers, the thermal efficiency of the alkaline electrolyser model can be calculated. When using the waste heat, a thermal efficiency of 92.83 % can be achieved.

Unfortunately, the current alkaline electrolysers do not use plate heat exchangers. Most alkaline electrolysers make use of cooling by an air heat exchanger. Therefore, research into the heat that gets released when making use of an air cooled heat exchanger is of interest. The air can be used in a heat network, though the current alkaline electrolysers are already in use and possibly not near a heat network. Therefore, the hot air could be used for heating purposes in the nearby area. An example could be the heating of a swimming pool. The hot air outlet of the alkaline electrolyser can be used to warm the water of the swimming pool. For the heating of the water of the pool a shell & tube heat exchanger can be used. To look at this scenario a shell & tube heat exchanger is added to the ASPEN model as can be seen in figure 36.

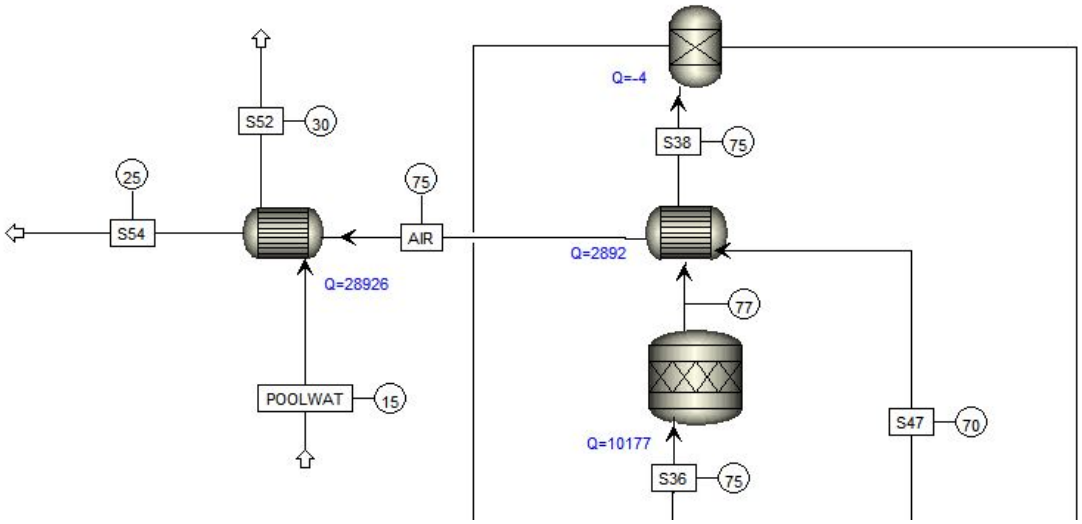

Figure 36: ASPEN model with shell & tube HEX for swimming pool.

The output temperature of the water is equal to 30 °C, which is, according to literature, a good temperature to swim [91]. The output of the ASPEN model for the shell & tube heat exchanger is shown in table 36.

Table 9: Shell & tube HEX implemented in the ASPEN model for air-water heating for a swimming pool.

Variable	**Shell & tube HEX**
Total power stack [kW]	122.1
Fluid	Air
Flowrate [kg/h]	1700
Length [m]	2.850
Width [m]	0.257
Cost [$]	12880

The resulted efficiency loss of the shell & tube heat exchanger is equal to 16.6 %. For an alkaline electrolyser with a stack of 122.1 kW, 1700 kg/h of water can be heated to 30 °C. However, this does not include the losses that occur by transferring the hot air from the alkaline electrolyser to the swimming pool. Losses of 25 % need to be calculated into the final result. Therefore, 1275 kg/h water can be heated up to 30 °C. An olympic pool has a volume of 2500 m^3, this can be filled by 2,492,500 kg water [92]. Therefore, 1954.9 hours are needed to heat all the water, which is equal to 81.45 days. Next to this, the costs for the shell & tube heat exchanger are equal to $ 12,880. Which is assumed as not desirable. Assuming a load of 50 %, an alkaline electrolyser of 19.89 MW is needed to heat the swimming pool in one day.

When a pool is already in use the thermal energy demand is for keeping the pool at a certain temperature. The total thermal power demand, $\dot{Q}_{tot}$, of an indoor pool is shown in equation 68 [93].

$$\dot{Q}_{tot} = \dot{Q}_{\text{evap}} + \dot{Q}_{cond} + \dot{Q}_{conv} + \dot{Q}_{rad} + \dot{Q}_{renov} \tag{68}$$

$\dot{Q}_{\text{evap}}$ represents the thermal demand due to evaporation, $\dot{Q}_{cond}$ represents the thermal demand due to conduction, $\dot{Q}_{conv}$ represents the thermal demand due to convection, $\dot{Q}_{rad}$ represents the thermal demand

due to radiation and $\dot{Q}_{renov}$ represents the thermal demand for continuously renewing the water. The water needs to be renewed for sanitary reasons. Many different factors are of importance for the heating of an indoor pool. Since a detailed model of the swimming pool is out of scope, a back-of-the-envelope estimation is made of the thermal power demand, based on literature. The thermal power demand of a semi Olympic pool (half of a real Olympic pool) is equal to 369.4 MWh/year. The assumption is made that for an Olympic pool, of twice the size, the thermal energy demand will be equal to 738.7 MWh/year [93]. To calculate the mass flow needed for the heating of the pool equation 15 is used. Which results in a water flow of 6.076 m^3/h, which is equal to 6067 kg/h. In conclusion, assuming a load of 50 %, an alkaline electrolyser of 1.16 MW is needed to keep an Olympic swimming pool on temperature.

6 Discussion

This chapter is intended to discuss different factors which could be of influence on the output of the model.

6.1 Operating temperature

There are several factors which could be of influence on the output of the model. One of those factors is the operating temperature. The influence of the operating temperature on the cell voltage is shown in figure 37.

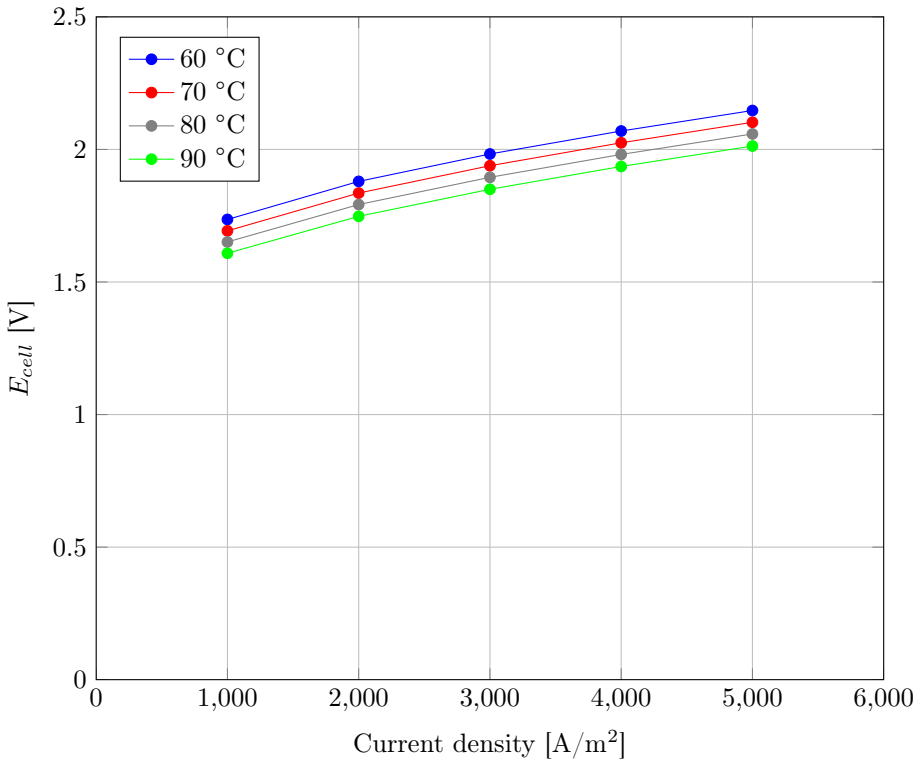

Figure 37: The influence of temperature on E_{cell}.

At 90 °C the cell voltage is low and the thermal efficiency is therefore high. An alkaline electrolyser operates at temperatures lower than 90 °C due to the decrease of the corrosion resistance of the electrolyser components at higher temperatures. At higher temperatures the alkaline electrolyser will have a shorter life span. A second reason is that at higher temperatures more water will be evaporated and therefore the purity of the produced hydrogen will lower [94]. Nevertheless, experiments are carried out to study the behaviour of the model when operating at 90 °C instead of operation at 75 °C.

At 90 °C the voltage efficiency is equal to 75.8 %, the electrical efficiency is 74.9 % and the system efficiency is 74.8 %. These efficiencies are higher than for the system operating at 75 °C, as expected. $Q_{generated}$ is 2377.3 W per stack of cells and Q_{cooled} is 2269.0 W per stack of cells. Therefore, Q_{loss} is 108.00 W per stack of cells. When using the waste heat and assuming transport losses of 25 %, the thermal efficiency of the alkaline electrolyser at 90 °C is equal to 92.99 %. This is almost equal to the system operating at 75 °C.

6.2 Seasonal effects

For the cooling water and cooling air fixed temperatures are taken. However, the temperature of air is not constant and differs every day. The same goes for water temperatures. The influence of seasonal effects on the air and water temperature are shown in figure 38 and figure 39. The effects of the varying temperature on the flowrate of the cooling fluid are displayed in the same figures in the graphs on the right.

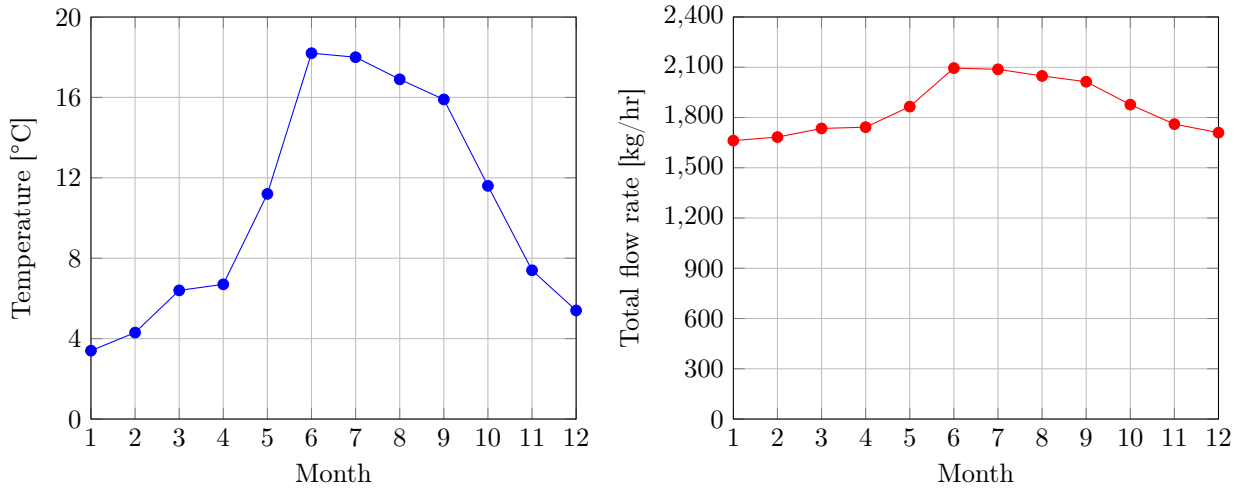

Figure 38: Seasonal fluctuations air temperature the Netherlands and the influence on the flowrate for the cooling of an alkaline electrolyser stack consisting of 12 stacks of cells [95].

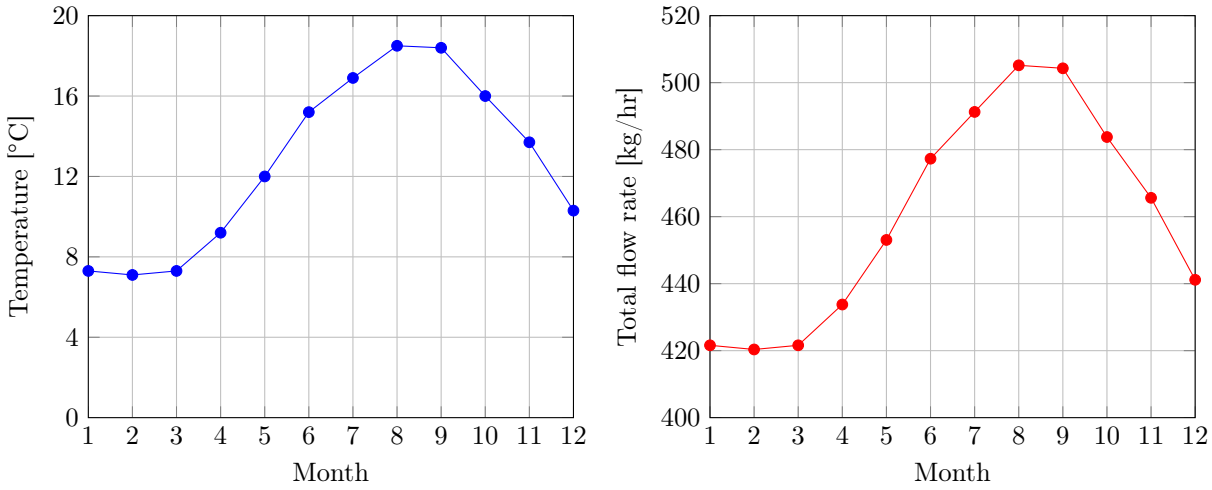

Figure 39: Seasonal fluctuations water temperature of the North sea and the influence on the flowrate for the cooling of an alkaline electrolyser stack consisting of 12 stacks of cells [96].

The fluctuations in the flowrate of the coolant, due to seasonal effects, are rather small. From the water cooling mean flowrate a maximum deviation of 10 % is found. For cooling with air the deviation has a maximum of 13 %.

6.3 Steady state model

The alkaline electrolyser is modelled as a steady state model. The source of electricity for the production of green hydrogen is coming from renewable energy sources. Therefore, the input for an alkaline electrolyser for the production of green hydrogen is dynamic. For this model constant variables are assumed.

6.4 Recycle stream

In an alkaline electrolyser the water and KOH are recycled and used again. Considering that the ASPEN model is modelled as a steady state model, no recycle streams have been added. A water deficit is added in the model such that the water value stays on 900 kg/h and a mixer and pump are present so that the output stream could be recycled and all the correct equipment is modelled in the ASPEN model. The lack of the recycle stream is not considered as of any importance to the outcome of this research.

6.5 Steady pressure

In the model a steady pressure in the electrolyser stack is assumed. The pressure normally increases during the process. This is not modelled because pressure is of almost no influence on the system. The influence of pressure on E_{cell} is shown in figure 40.

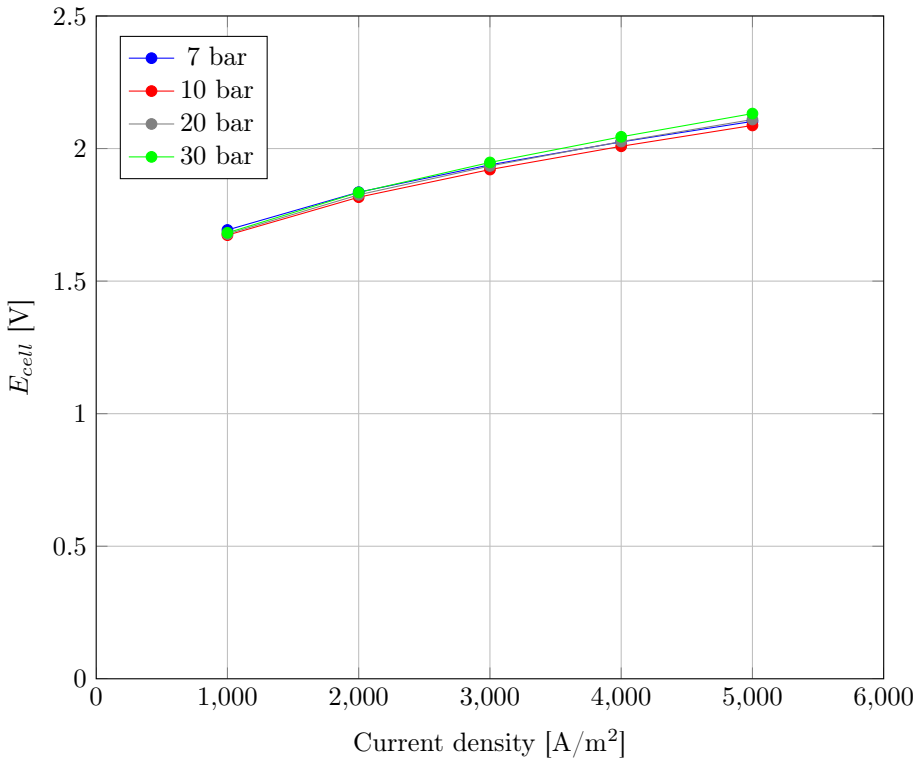

Figure 40: The influence of pressure on E_{cell}.

6.6 Input parameters

Some values from table 1 are in contrast with the values mentioned earlier. The differences are small, but present. In different papers different values are mentioned. The influence of temperature and pressure on the model have already been researched. An option is to research all input values. For example, a sensitivity analyses has been carried out to study the influence of varying power on the heat output. The result is shown in figure 41. According to the figure, a lower stack power results in a lower cooling water temperature.

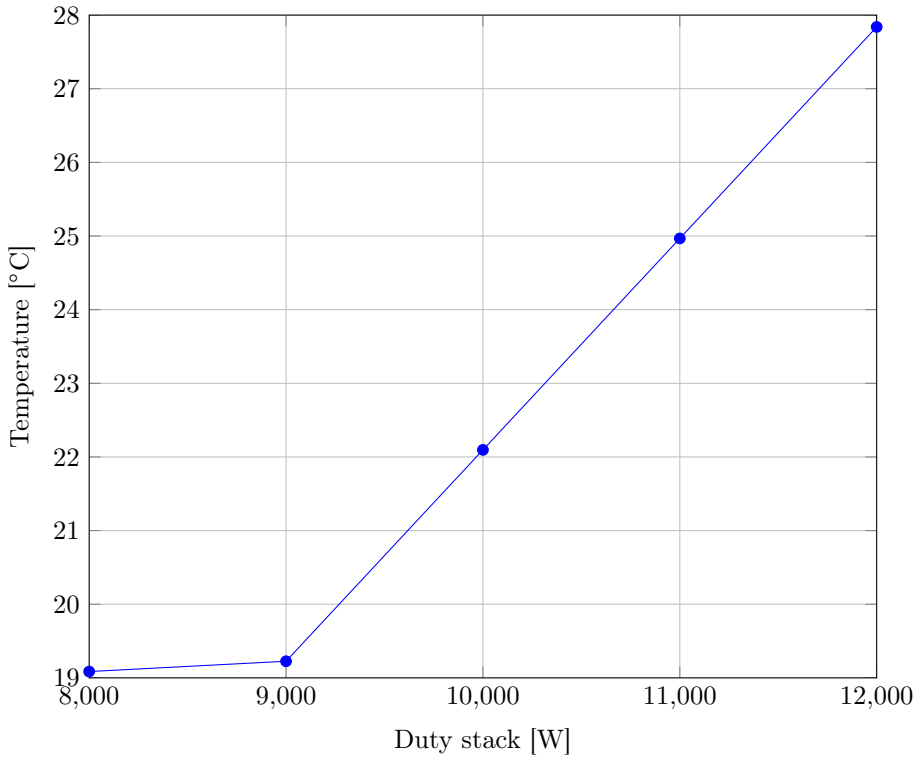

Figure 41: Sensitivity curve: influence of changing duty on temperature cool water stream.

7 Conclusion

To conclude, in this research the possibility of using the heat that gets released during the production of green hydrogen using an alkaline electrolyser, is investigated on the basis of the following research question and subquestions.

Research question:
Is it possible to use the heat released during the production of green hydrogen using alkaline water electrolysis?

Subquestions:

- How much heat does an alkaline electrolyser produce when producing green hydrogen?
- How much of the heat can, in theory, be recovered from the process?
- What is the temperature of the heat recovered from the process?
- What heat recovery system can best be used to recover the heat?
- What possible applications are there for the use of the excess heat?
- Which of the possible applications for the use of the excess heat is considered most profitable and why?

A model of an alkaline electrolyser has been developed in ASPEN Plus to answer the research question and subquestions. The model consists of an electrochemical model, thermal model and cooling system. The hydrogen production output of the model has been compared with an alkaline electrolyser developed by the company Nel hydrogen to determine if the model is a realistic representation of an alkaline electrolyser. A difference of 13.49 % was found between the output of the alkaline electrolyser from Nel hydrogen and the model in ASPEN. The difference of 13.49 % is assumed a realistic value and therefore the model is accepted. The ASPEN model produces hydrogen of a purity of 99.84 vol.%. The thermal efficiency of the model is equal to 73.3 %. The generated heat is equal to 26.7 % of the overall power of the stack. From this 26.7 % 0.66 % is lost. The rest of the heat needs to be cooled. To determine which heat exchanger is best to use for recovering the heat of the alkaline electrolyser, three different designs have been implemented in the ASPEN model. A plate heat exchanger, an air cooled heat exchanger and a shell & tube heat exchanger. The plate heat exchanger is the cheapest and smallest heat exchanger and therefore the best choice for recovering the waste heat. The model operates at 75 °C, therefore the maximum output of the plate heat exchanger water output stream is also equal to 75 °C. When more heat is produced, a bigger cooling fluid stream is needed.

If the heat released during electrolysis can be used, depends on the location of the electrolyser. Heat from an alkaline electrolyser can best be transported by a medium temperature heat network. In a medium temperature heat network heat is directly supplied for both space heating and hot tap water. To minimize losses a heat network needs to be close by. Practice shows that heat networks have losses of around 20-30 % on an annual basis. There are several locations where a connection to a heat network is possible. However, using the heat from the alkaline electrolyser model is not an option, when the electrolyser is located offshore. When connecting the alkaline electrolyser to a heat network, a 2 MW electrolyser, working 50 % of the time, can provide heat for 628 households. When assuming transport losses of 25 % and the use of plate heat exchangers, a thermal efficiency of the alkaline electrolyser model of 92.83 % can be achieved when using the waste heat.

8 Recommendations

During this research some simplifications have been made and some aspects of the problem have not been researched. In this chapter recommendations for follow-up research will be discussed. The first part consists of more in-depth research recommendations, while the second part consists of recommendations for research related to the topic, but in a different direction.

8.1 Recommendations model

- To model the stack as realistically as possible the model of Ulleberg and Sanchez et al. was used. This model has been validated and used in many scientific papers. Nevertheless, it is recommended to research and test a real alkaline electrolyser. This gives the opportunity to measure the heat output and hydrogen output experimentally. The model in ASPEN is a steady state model. When using a real alkaline electrolyser it is possible to take into account the dynamic behaviour of the system and the influence of the varying loads.
- Temperature is of significant influence regarding the efficiency of the model. The influence of higher operating temperatures on the ageing of the alkaline electrolyser and the quality of the hydrogen produced has not been researched. When higher operating temperatures for alkaline electrolysis are desired it is recommended to first research this influence.
- In alkaline electrolysis water is used for the production of hydrogen. No further research has been done regarding this water. It is assumed that the water used is available and of good quality. More in depth research needs to be carried out to determine what water quality is needed and if this water can be easily used. Also the influence of drought could be interesting to take into account as well as the influence of the location of the alkaline electrolyser.
- No in depth research has been done into the cooling fluid. The options of water and air were modelled for different heat exchangers. Based on findings in literature, water was chosen as cooling fluid. More elaborate research into different cooling fluids could be useful.
- Research for using a heat pump in combination with the cooling water output flow has not been carried out. The cooling stream achieves a high enough temperature for the medium temperature heat network. A heat pump in combination with the alkaline electrolyser model could be useful when higher output temperatures are desired. When higher output temperatures are desired, follow-up research is recommended.
- In this research the focus was on retrieving the heat produced at the stack. However, there is also a small amount of heat produced at the H_2O traps. In future research the possibility and efficiency of recovering heat released at the H_2O traps can be investigated as well. Although, these values are relatively low, namely, 3.61 % of the total generated heat of the system. Therefore, recovering this heat will only be of small influence on the overall system efficiency.

8.2 Recommendations topic related research

- This study was conducted for an alkaline electrolyser. The use of heat released during the production of green hydrogen using a PEM electrolyser or a SOEC is as well of interest. The heat released by a PEM electrolyser will be around the same amount as for an alkaline electrolyser. A SOEC will

give a different output because of the high operating temperature and different system configuration. Therefore, it is recommended to conduct research into the use of heat released during the production of green hydrogen using a SOEC.

- In this thesis the use of heat released during the production of green hydrogen using an alkaline electrolyser was quantified. No research was carried out regarding the oxygen output. The oxygen released is still wasted in the current model. For follow-up research a focus on the wasted oxygen is recommended.

References

[1] NEL hydrogen. (2022). *Atmospheric alkaline electrolyser* [Last accessed: 18-05-2022]. https://nelhydrogen.com/product/atmospheric-alkaline-electrolyser-a-series/

[2] United Nations. (2021). *Climate and weather related disasters surge five-fold over 50 years, but early warnings save lives - wmo report.* [Last accessed: 09-11-2021]. https://news.un.org/en/story/2021/09/1098662

[3] Smil, V. (2016). *Energy transitions: Global and national perspectives*. ABC-CLIO.

[4] Dale, S. (2019). BP statistical review of world energy. *BP Plc, London, United Kingdom*, 14–16.

[5] International Energy Agency. (2019a). *Hydrogen.* [Last accessed: 31-10-2021]. https://www.iea.org/fuels-and-technologies/hydrogen

[6] Sørensen, B., & Spazzafumo, G. (2018). Hydrogen and fuel cells (third edition). In B. Sørensen & G. Spazzafumo (Eds.). Academic Press. https://doi.org/https://doi.org/10.1016/B978-0-08-100708-2.00003-5

[7] California Hydrogen Business Council. (2015). Power to gas: The case for hydrogen white paper [Last accessed: 15-11-2021]. https://www.californiahydrogen.org/wp-content/uploads/2018/01/CHBC-Hydrogen-Energy-Storage-White-Paper-FINAL.pdf

[8] Züttel, A., Remhof, A., Borgschulte, A., & Friedrichs, O. (2010). Hydrogen: The future energy carrier. *Philosophical Transactions: Mathematical, Physical and Engineering Sciences*, *368*(1923), 3329–3342. http://www.jstor.org/stable/25699171

[9] Tzimas, E., Filiou, C., Peteves, S., & Veyret, J. (2003). Hydrogen storage: State-of-the-art and future perspective. *EU Commission, JRC Petten, EUR 20995EN*.

[10] Newborough, M., & Cooley, G. (2020). Developments in the global hydrogen market: The spectrum of hydrogen colours. *Fuel Cells Bulletin*, *2020*(11), 16–22. https://doi.org/https://doi.org/10.1016/S1464-2859(20)30546-0

[11] Worldometer. (2017). *Co2 emissions by country* [Last accessed: 05-05-2022]. https://www.worldometers.info/co2-emissions/co2-emissions-by-country/

[12] Howarth, R. W., & Jacobson, M. Z. (2021). How green is blue hydrogen? *Energy Science & Engineering*. https://doi.org/https://doi.org/10.1002/ese3.956

[13] Dincer, I. (2012). Green methods for hydrogen production. *International Journal of Hydrogen Energy*, *37*(2), 1954–1971. https://doi.org/https://doi.org/10.1016/j.ijhydene.2011.03.173

[14] Zeng, K., & Zhang, D. (2010). Recent progress in alkaline water electrolysis for hydrogen production and applications. *Progress in Energy and Combustion Science*, *36*(3), 307–326. https://doi.org/https://doi.org/10.1016/j.pecs.2009.11.002

[15] Meza, E. (2022). *Rising gas prices make green hydrogen cheaper than grey hydrogen* [Last accessed: 15-05-2022]. https://www.cleanenergywire.org/news/rising-gas-prices-make-green-hydrogen-cheaper-gray-hydrogen

[16] Rashid, M., Al Mesfer, M. K., Naseem, H., & Danish, M. (2015). Hydrogen production by water electrolysis: A review of alkaline water electrolysis, pem water electrolysis and high temperature water electrolysis. *International Journal of Engineering and Advanced Technology*.

[17] Balat, M. (2008). Potential importance of hydrogen as a future solution to environmental and transportation problems. *International Journal of Hydrogen Energy*, *33*(15), 4013–4029. https://doi.org/https://doi.org/10.1016/j.ijhydene.2008.05.047

[18] McPhy. (2021). *Hydeal ambition*. [Last accessed: 16-09-2021]. https://mcphy.com/en/news/hydeal-ambition/?cn-reloaded=1

[19] Collins, L. (2021). *Global green-hydrogen pipeline exceeds 250gw — here's the 27 largest gigawatt-scale projects*. [Last accessed: 18-09-2021]. https://www.rechargenews.com/energy-transition/global-green-hydrogen-pipeline-exceeds-250gw-heres-the-27-largest-gigawatt-scale-projects/2-1-933755

[20] Gasunie. (2021). *Overview of hydrogen projects in the netherlands*. [Last accessed: 09-10-2021]. https://www.topsectorenergie.nl/tki-nieuw-gas/innovatieprogramma/waterstof-een-robuust-element-de-energietransitie

[21] International Energy Agency. (2019b). *Renewables 2019*. [Last accessed: 19-10-2021]. https://www.iea.org/reports/renewables-2019

[22] Stempien, J. P., Liu, Q., Ni, M., Sun, Q., & Chan, S. H. (2014). Physical principles for the calculation of equilibrium potential for co-electrolysis of steam and carbon dioxide in a solid oxide electrolyzer cell (soec). *Electrochimica Acta*, *147*, 490–497. https://doi.org/https://doi.org/10.1016/j.electacta.2014.09.144

[23] Brown, T. L., LeMay, H. E., Bursten, B. E., & Brunauer, L. S. (1997). *Chemistry: The central science* (Vol. 13). Prentice Hall Englewood Cliffs, NJ.

[24] Godula-Jopek, A. (2015). *Hydrogen production: By electrolysis*. John Wiley & Sons.

[25] Fabbri, E., Habereder, A., Waltar, K., Kötz, R., & Schmidt, T. J. (2014). Developments and perspectives of oxide-based catalysts for the oxygen evolution reaction. *Catalysis, Science & Technology*, *4*, 3800–3821. https://doi.org/http://dx.doi.org/10.1039/C4CY00669K

[26] Cossar, E., Oyarce Barnett, A., Seland, F., & Baranova, E. A. (2019). The performance of nickel and nickel-iron catalysts evaluated as anodes in anion exchange membrane water electrolysis. *Catalysts*, *9*(10). https://doi.org/10.3390/catal9100814

[27] Ursua, A., Gandia, L. M., & Sanchis, P. (2012). Hydrogen production from water electrolysis: Current status and future trends. *Proceedings of the IEEE*, *100*(2), 410–426. https://doi.org/10.1109/JPROC.2011.2156750

[28] Dincer, I., & Zamfirescu, C. (2016). *Sustainable hydrogen production* (I. Dincer & C. Zamfirescu, Eds.). Elsevier. https://doi.org/https://doi.org/10.1016/B978-0-12-801563-6.00007-8

[29] Roy, A., Watson, S., & Infield, D. (2006). Comparison of electrical energy efficiency of atmospheric and high-pressure electrolysers. *International Journal of Hydrogen Energy*, *31*(14), 1964–1979. https://doi.org/https://doi.org/10.1016/j.ijhydene.2006.01.018

[30] Ayers, K. E., Anderson, E. B., Capuano, C., Carter, B., Dalton, L., Hanlon, G., Manco, J., & Niedzwiecki, M. (2019). Research advances towards low cost, high efficiency PEM electrolysis. *ECS Transactions*, *33*(1), 3–15. https://doi.org/10.1149/1.3484496

[31] Abdin, Z., Webb, C., & Gray, E. (2017). Modelling and simulation of an alkaline electrolyser cell. *Energy*, *138*, 316–331. https://doi.org/https://doi.org/10.1016/j.energy.2017.07.053

[32] Coutanceau, C., Baranton, S., & Audichon, T. (2018). *Hydrogen electrochemical production* (C. Coutanceau, S. Baranton, & T. Audichon, Eds.). Academic Press. https://doi.org/https://doi.org/10.1016/B978-0-12-811250-2.00001-7

[33] Vincent, I., & Bessarabov, D. (2018). Low cost hydrogen production by anion exchange membrane electrolysis: A review. *Renewable and Sustainable Energy Reviews*, *81*, 1690–1704. https://doi.org/https://doi.org/10.1016/j.rser.2017.05.258

[34] David, M., Ocampo-Martínez, C., & Sánchez-Peña, R. (2019). Advances in alkaline water electrolyzers: A review. *Journal of Energy Storage*, *23*, 392–403. https://doi.org/https://doi.org/10.1016/j.est.2019.03.001

[35] Jang, D., Cho, H.-S., & Kang, S. (2021). Numerical modeling and analysis of the effect of pressure on the performance of an alkaline water electrolysis system. *Applied Energy*, *287*, 116554. https://doi.org/https://doi.org/10.1016/j.apenergy.2021.116554

[36] Shiva Kumar, S., & Himabindu, V. (2019). Hydrogen production by pem water electrolysis – a review. *Materials Science for Energy Technologies*, *2*(3), 442–454. https://doi.org/https://doi.org/10.1016/j.mset.2019.03.002

[37] Schmidt, O., Gambhir, A., Staffell, I., Hawkes, A., Nelson, J., & Few, S. (2017). Future cost and performance of water electrolysis: An expert elicitation study. *International Journal of Hydrogen Energy*, *42*(52), 30470–30492. https://doi.org/https://doi.org/10.1016/j.ijhydene.2017.10.045

[38] Sapountzi, F. M., Gracia, J. M., Weststrate, C., Fredriksson, H. O., & Niemantsverdriet, J. (2017). Electrocatalysts for the generation of hydrogen, oxygen and synthesis gas. *Progress in Energy and Combustion Science*, *58*, 1–35. https://doi.org/https://doi.org/10.1016/j.pecs.2016.09.001

[39] Bhandari, R., Trudewind, C. A., & Zapp, P. (2014). Life cycle assessment of hydrogen production via electrolysis – a review. *Journal of Cleaner Production*, *85*, 151–163. https://doi.org/https://doi.org/10.1016/j.jclepro.2013.07.048

[40] Grigoriev, S., Fateev, V., Bessarabov, D., & Millet, P. (2020). Current status, research trends, and challenges in water electrolysis science and technology. *International Journal of Hydrogen Energy*, *45*(49), 26036–26058. https://doi.org/https://doi.org/10.1016/j.ijhydene.2020.03.109

[41] Manabe, A., Kashiwase, M., Hashimoto, T., Hayashida, T., Kato, A., Hirao, K., Shimomura, I., & Nagashima, I. (2013). Basic study of alkaline water electrolysis. *Electrochimica Acta*, *100*, 249–256. https://doi.org/https://doi.org/10.1016/j.electacta.2012.12.105

[42] Carmo, M., Fritz, D. L., Mergel, J., & Stolten, D. (2013). A comprehensive review on pem water electrolysis. *International Journal of Hydrogen Energy*, *38*(12), 4901–4934. https://doi.org/https://doi.org/10.1016/j.ijhydene.2013.01.151

[43] Abdin, Z., Webb, C., & Gray, E. (2015). Modelling and simulation of a proton exchange membrane (pem) electrolyser cell. *International Journal of Hydrogen Energy*, *40*(39), 13243–13257. https://doi.org/https://doi.org/10.1016/j.ijhydene.2015.07.129

[44] Danilovic, N., Ayers, K. E., Capuano, C., Renner, J. N., Wiles, L., & Pertoso, M. (2016). (plenary) challenges in going from laboratory to megawatt scale PEM electrolysis. *ECS Transactions*, *75*(14), 395–402. https://doi.org/10.1149/07514.0395ecst

[45] Gandía, L. M., Arzamendi, G., & Diéguez, P. M. (2013). *Renewable hydrogen technologies*. Elsevier. https://doi.org/https://doi.org/10.1016/B978-0-444-56352-1.00015-5

[46] Ozturk, M., & Dincer, I. (2021). A comprehensive review on power-to-gas with hydrogen options for cleaner applications. *International Journal of Hydrogen Energy*, *46*(62), 31511–31522. https://doi.org/https://doi.org/10.1016/j.ijhydene.2021.07.066

[47] Nie, J., Chen, Y., Boehm, R. F., & Katukota, S. (2008). A Photoelectrochemical Model of Proton Exchange Water Electrolysis for Hydrogen Production. *Journal of Heat Transfer*, *130*(4). https://doi.org/10.1115/1.2789722

[48] Ni, M., Leung, M. K., & Leung, D. Y. (2008). Technological development of hydrogen production by solid oxide electrolyzer cell (soec). *International Journal of Hydrogen Energy*, *33*(9), 2337–2354. https://doi.org/https://doi.org/10.1016/j.ijhydene.2008.02.048

[49] Flowers, P., Theopold, K., Langley, R., Robinson, W. R. et al. (2015). Chemistry: Openstax.

[50] Amores, E., Sánchez, M., Rojas, N., & Sánchez-Molina, M. (2021). Sustainable fuel technologies handbook. In S. Dutta & C. Mustansar Hussain (Eds.). Academic Press. https://doi.org/https://doi.org/10.1016/B978-0-12-822989-7.00010-X

[51] Jouhara, H., Khordehgah, N., Almahmoud, S., Delpech, B., Chauhan, A., & Tassou, S. A. (2018). Waste heat recovery technologies and applications. *Thermal Science and Engineering Progress*, *6*, 268–289. https://doi.org/https://doi.org/10.1016/j.tsep.2018.04.017

[52] Brückner, S., Liu, S., Miró, L., Radspieler, M., Cabeza, L. F., & Lävemann, E. (2015). Industrial waste heat recovery technologies: An economic analysis of heat transformation technologies. *Applied Energy*, *151*, 157–167. https://doi.org/https://doi.org/10.1016/j.apenergy.2015.01.147

[53] Quoilin, S., Broek, M. V. D., Declaye, S., Dewallef, P., & Lemort, V. (2013). Techno-economic survey of organic rankine cycle (orc) systems. *Renewable and Sustainable Energy Reviews*, *22*, 168–186. https://doi.org/https://doi.org/10.1016/j.rser.2013.01.028

[54] Perko, J., Dugec, V., Topic, D., Sljivac, D., & Kovac, Z. (2011). Calculation and design of the heat pumps. *Proceedings of the 2011 3rd International Youth Conference on Energetics (IYCE)*, 1–7.

[55] Get H2 group. (2021). *Get h2 lingen*. [Last accessed: 12-10-2021]. https://www.get-h2.de/en/project-lingen/

[56] GROHW. (2021). *Wat is waterstof?*. [Last accessed: 16-10-2021]. https://grohw.nl/wat-is-waterstof/

[57] Tiktak, W. (2019). *Heat management of pem electrolysis: A study on the potential of excess heat from medium to largescale pem electrolyisis and the performance analysis of a dedicated cooling system* (Master's thesis). Delft University of Technology. https://repository.tudelft.nl/islandora/object/uuid%5C%3Ac046820a-72bc-4f05-b72d-e60a3ecb8c89?collection=education

[58] Wang, F., Wang, L., Ou, Y., Lei, X., Yuan, J., Liu, X., & Zhu, Y. (2021). Thermodynamic analysis of solid oxide electrolyzer integration with engine waste heat recovery for hydrogen production. *Case Studies in Thermal Engineering*, *27*, 101240. https://doi.org/https://doi.org/10.1016/j.csite.2021.101240

[59] Michigan State University. (2021). Aspen tutorial [Last accessed: 26-11-2021]. https://www.chems.msu.edu/resources/tutorials/ASPEN

[60] Adams II, T. A. (2018). *Learn aspen plus in 24 hours*. McGraw-Hill Ed. https://www.accessengineeringlibrary.com/content/book/9781260116458

[61] Sánchez, M., Amores, E., Abad, D., Rodríguez, L., & Clemente-Jul, C. (2020). Aspen plus model of an alkaline electrolysis system for hydrogen production. *International Journal of Hydrogen Energy*, *45*(7), 3916–3929. https://doi.org/https://doi.org/10.1016/j.ijhydene.2019.12.027

[62] Santos, D., Sequeira, C., & Figueiredo, J. (2012). Hydrogen production by alkaline water electrolysis. *Química Nova*, *36*, 1176–1193. https://doi.org/10.1590/S0100-40422013000800017

[63] Evans, J. (2012). *Pump efficiency—what is efficiency?* [Last accessed: 05-05-2022]. https://www.pumpsandsystems.com/pump-efficiency-what-efficiency#:~:text=Many%5C%20medium%5C%20and%5C%20larger%5C%20centrifugal,break%5C%20the%5C%2090%5C%20percent%5C%20barrier.

[64] Ulleberg, Ø. (2003). Modeling of advanced alkaline electrolyzers: A system simulation approach. *International Journal of Hydrogen Energy*, *28*(1), 21–33. https://doi.org/https://doi.org/10.1016/S0360-3199(02)00033-2

[65] Amores, E., Rodrıguez, J., Oviedo, J., & de Lucas-Consuegra, A. (2017). Development of an operation strategy for hydrogen production using solar pv energy based on fluid dynamic aspects. *Open Engineering*, *7*(1), 141–152.

[66] Bernadet, L., Gousseau, G., Chatroux, A., Laurencin, J., Mauvy, F., & Reytier, M. (2015). Influence of pressure on solid oxide electrolysis cells investigated by experimental and modeling approach. *International Journal of Hydrogen Energy*, *40*(38), 12918–12928. https://doi.org/https://doi.org/10.1016/j.ijhydene.2015.07.099

[67] Ni, M. (2010). Modeling of a solid oxide electrolysis cell for carbon dioxide electrolysis. *Chemical Engineering Journal*, *164*(1), 246–254. https://doi.org/https://doi.org/10.1016/j.cej.2010.08.032

[68] García-Valverde, R., Espinosa, N., & Urbina, A. (2012). Simple pem water electrolyser model and experimental validation [10th International Conference on Clean Energy 2010]. *International Journal of Hydrogen Energy*, *37*(2), 1927–1938. https://doi.org/https://doi.org/10.1016/j.ijhydene.2011.09.027

[69] Guidelli, R., Compton, R. G., Feliu, J. M., Gileadi, E., Lipkowski, J., Schmickler, W., & Trasatti, S. (2014). Defining the transfer coefficient in electrochemistry: An assessment (iupac technical report). *Pure and Applied Chemistry*, *86*(2), 245–258. https://doi.org/https://doi.org/10.1515/pac-2014-5026

[70] Dickinson, E. J., & Wain, A. J. (2020). The butler-volmer equation in electrochemical theory: Origins, value, and practical application. *Journal of Electroanalytical Chemistry*, *872*, 114145. https://doi.org/https://doi.org/10.1016/j.jelechem.2020.114145

[71] Kear, G., & Walsh, F. (2005). The characteristics of a true tafel slope. *Corrosion and Materials*, *30*(6), 51–55. https://eprints.soton.ac.uk/49025/

[72] van der Merwe, J., Uren, K., van Schoor, G., & Bessarabov, D. (2013). A study of the loss characteristics of a single cell pem electrolyser for pure hydrogen production. *2013 IEEE International Conference on Industrial Technology (ICIT)*, 668–672. https://doi.org/10.1109/ICIT.2013.6505751

[73] Johnson, P., & Babb, A. (1956). Liquid diffusion of non-electrolytes. *Chemical reviews*, *56*(3), 387–453.

[74] Sundén, B. (2019). Hydrogen, batteries and fuel cells. In B. Sundén (Ed.). Academic Press. https://doi.org/https://doi.org/10.1016/B978-0-12-816950-6.00003-8

[75] Sánchez, M., Amores, E., Rodríguez, L., & Clemente-Jul, C. (2018). Semi-empirical model and experimental validation for the performance evaluation of a 15 kw alkaline water electrolyzer. *International Journal of Hydrogen Energy*, *43*(45), 20332–20345. https://doi.org/https://doi.org/10.1016/j.ijhydene.2018.09.029

[76] Bejan, A., & Kraus, A. D. (2003). *Heat transfer handbook* (Vol. 1). John Wiley & Sons.

[77] Laurencin, J., Kane, D., Delette, G., Deseure, J., & Lefebvre-Joud, F. (2011). Modelling of solid oxide steam electrolyser: Impact of the operating conditions on hydrogen production. *Journal of Power Sources*, *196*(4), 2080–2093. https://doi.org/https://doi.org/10.1016/j.jpowsour.2010.09.054

[78] Patil, A., Radle, M., & Shome, B. (2015). One-dimensional solar heat load simulation model for a parked car. *SAE Technical Papers*, *2015*. https://doi.org/10.4271/2015-01-0356

[79] Sakas, G., Ibáñez-Rioja, A., Ruuskanen, V., Kosonen, A., Ahola, J., & Bergmann, O. (2022). Dynamic energy and mass balance model for an industrial alkaline water electrolyzer plant process. *International Journal of Hydrogen Energy*, *47*(7), 4328–4345. https://doi.org/https://doi.org/10.1016/j.ijhydene.2021.11.126

[80] Sinnott, R., & Towler, G. (2009). *Chemical engineering design*. Elsevier Science & Technology.

[81] Nel Hydrogen. (2022). *The world's most efficient and reliable electrolysers* [Last accessed: 09-05-2022]. https://nelhydrogen.com/wp-content/uploads/2022/01/Electrolysers-Brochure-Rev-D.pdf

[82] Sölken, W. (2022). *Air cooled heat exchangers* [Last accessed: 15-05-2022]. https://www.wermac.org/equipment/air-cooled_heatexchanger.html

[83] Parisher, R., & Rhea, R. (2012). Mechanical equipment. *Pipe drafting and Design*, *3*, 112–133.

[84] Mueller, P. (2019). *Overview of plate heat exchanger technology* [Last accessed: 15-05-2022]. https://academy.paulmueller.com/overview-of-plate-heat-exchanger-technology

[85] Edreis, E., & Petrov, A. (2020). Types of heat exchangers in industry, their advantages and disadvantages, and the study of their parameters. *IOP Conference Series: Materials Science and Engineering*, *963*(1), 012027. https://doi.org/10.1088/1757-899x/963/1/012027

[86] Infante Ferreira, C. (2020). *Course material equipment for heat & mass transfer* [Last accessed: 15-06-2022]. TU Delft course ME45165.

[87] Ministerie van Binnenlandse Zaken en Koninkrijksrelaties. (2020). *Staatsblad van het koninkrijk der nederlanden* [Last accessed: 09-05-2022]. https://zoek.officielebekendmakingen.nl/stb-2020-400.html

[88] TKI Urban Energy. (2020). *Warmtenetten* [Last accessed: 11-05-2022]. https://www.topsectorenergie.nl/tki-urban-energy/kennisdossiers/warmtenetten

[89] Stichting warmtenetwerk. (2022). *Warmteprojectentool* [Last accessed: 10-05-2022]. https://warmtenetwerk.nl/map/

[90] Eneco. (2022). *Wat is normaal verbruik?* [Last accessed: 31-03-2022]. https://www.eneco.nl/klantenservice/meters-meterstanden/normaal-verbruik/#:~:text=Het%5C%20gemiddelde%5C%20verbruik%5C%20van%5C%20warm,vergelijken%5C%20met%5C%20ongeveer%5C%2010%5C%20GJ.

[91] Zwembaden expert. (2016). *Wat is de ideale zwemwater temperatuur?* [Last accessed: 16-05-2022]. https://zwembadenexpert.nl/news/wat-is-de-ideale-zwemwater-temperatuur/

[92] Moak, J. (2022). *Olympic swimming pools* [Last accessed: 16-05-2022]. https://phinizycenter.org/olympic-swimming-pools/#:~:text=It%5C%20turns%5C%20out%5C%20that%5C%20Olympic,water%5C%20or%5C%20about%5C%20660%5C%2C000%5C%20gallons.

[93] Delgado Marín, J., Vera García, F., & García Cascales, J. (2019). Use of a predictive control to improve the energy efficiency in indoor swimming pools using solar thermal energy. *Solar Energy*, *179*, 380–390. https://doi.org/https://doi.org/10.1016/j.solener.2019.01.004

[94] Balabel, A., Zaky, M., & Sakr, I. (2014). Optimum operating conditions for alkaline water electrolysis coupled with solar pv energy system. *Arabian Journal for Science and Engineering*, *39*, 4211–4220. https://doi.org/10.1007/s13369-014-1050-6

[95] KNMI. (2021). *Weerstatistieken de bilt-2021* [Last accessed: 05-06-2022]. https://weerstatistieken.nl/

[96] Waar-Je-Zwemmen. (2022). *Wanneer kunt u gaan zwemmen in vlissingen in nederland (holland)* [Last accessed: 05-06-2022]. https://www.waar-je-zwemmen.nl/europa/nederland/vlissingen/when.html

Appendices

A Dutch green hydrogen initiatives

In table 10 an overview is shown of several green hydrogen production initiatives in the Netherlands. For many projects details are still vague or unknown.

Table 10: Dutch green hydrogen production initiatives [20].

Name	**Power [MW]**	**Hydrogen production [tonnes/year]**
DJewels-1	20	3000
Hydrogen Delta	1000	-
H2.50	250	45000
Eemshydrogen	50	-
Hy4Am	10	1752
GreenH2UB	10	-
HEAVENN	-	-
GZI NEXT	-	-
Bio Energy Netherlands	-	-
Hydrogen Gas Turbine Retrofit	-	-
Hydrogen mill	2	-
PosHYdon	1	-
H2ermes	100	-
Hydrogen from Organic Waste	-	-
NortH2	4000	800000
H2GO	2.5	-
HyNetherlands	100	-
GldH2	1	-
Hydrogen Mill Sint Philipsland	-	-
Energiepark Eemshaven-West	10	-
ELYgator	200	-
H2 conversion park	2	-
H2gate	-	-
H2ero	150	-
MULTIPLHY	-	-
BrigH2	50	-
Haddock	100	-
SeaH2Land	1000	-
H2Agro	-	-
CurtHyl	10	-
VoltH2	25	-
Uniper	100	-
The Rotterdam Electrolyser	200	-
Hydrohub GW	>1000	-
GROHW	-	-
H2ARVESTER	-	-

B Heat exchangers

In figure 42 the air cooled heat exchanger, designed by ASPEN EDR, is shown. In figure 43 and figure 44 the shell & tube heat exchanger designed by ASPEN EDR is shown. Figure 44 presents the tube sheet layout.

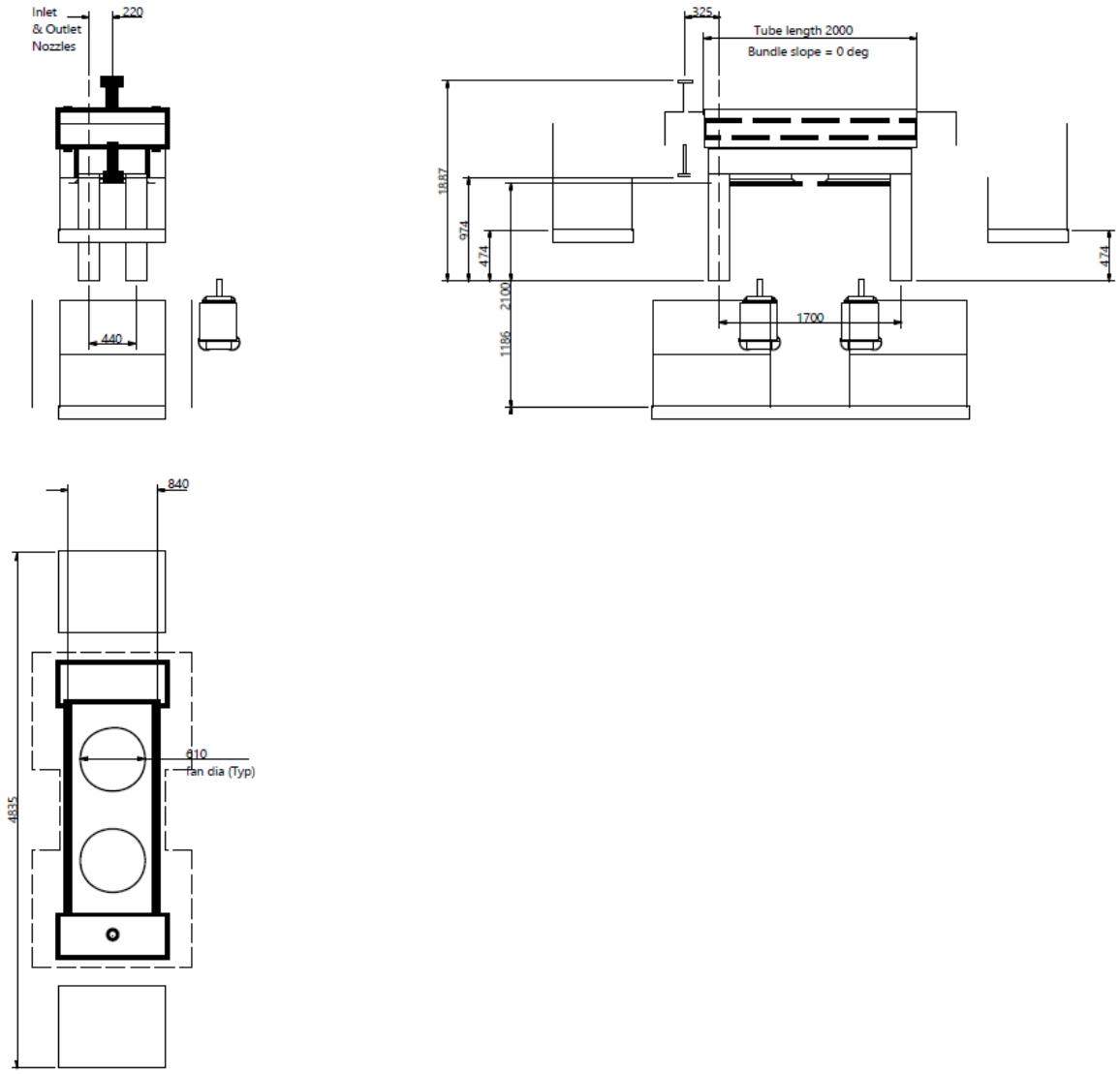

Figure 42: ASPEN model output air cooled heat exchanger.

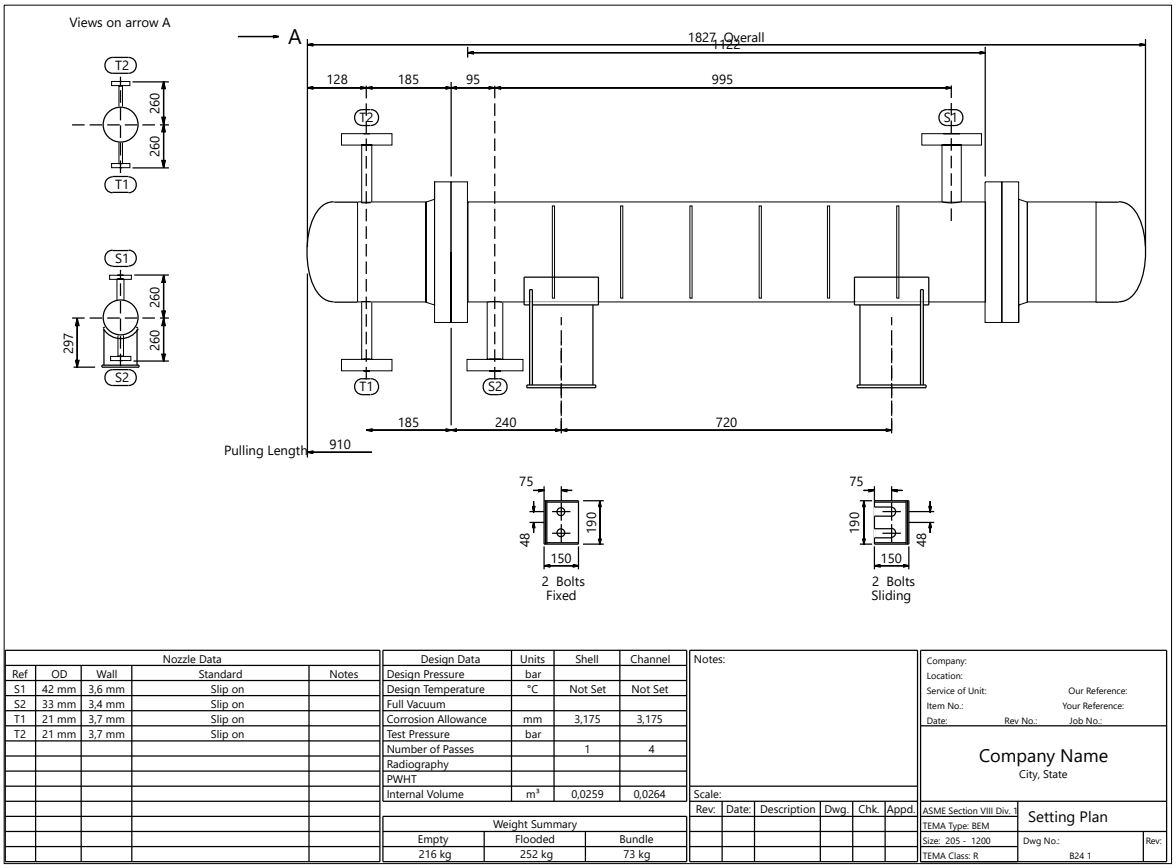

Nozzle Data				
Ref	OD	Wall	Standard	Notes
S1	42 mm	3,6 mm	Slip on	
S2	33 mm	3,4 mm	Slip on	
T1	21 mm	3,7 mm	Slip on	
T2	21 mm	3,7 mm	Slip on	

Design Data	Units	Shell	Channel
Design Pressure	bar		
Design Temperature	°C	Not Set	Not Set
Full Vacuum			
Corrosion Allowance	mm	3,175	3,175
Test Pressure	bar		
Number of Passes		1	4
Radiography			
PWHT			
Internal Volume	m³	0,0259	0,0264

Weight Summary		
Empty	Flooded	Bundle
216 kg	252 kg	73 kg

Notes:

Scale:

Rev:	Date:	Description	Dwg.	Chk.	Appd.

Company:
Location:
Service of Unit: Our Reference:
Item No.: Your Reference:
Date: Rev No.: Job No.:

Company Name
City, State

ASME Section VIII Div. 1
TEMA Type: BEM
Size: 205 - 1200
TEMA Class: R

Setting Plan

Dwg No.: B24.1 Rev:

Figure 43: ASPEN model output shell & tube heat exchanger.

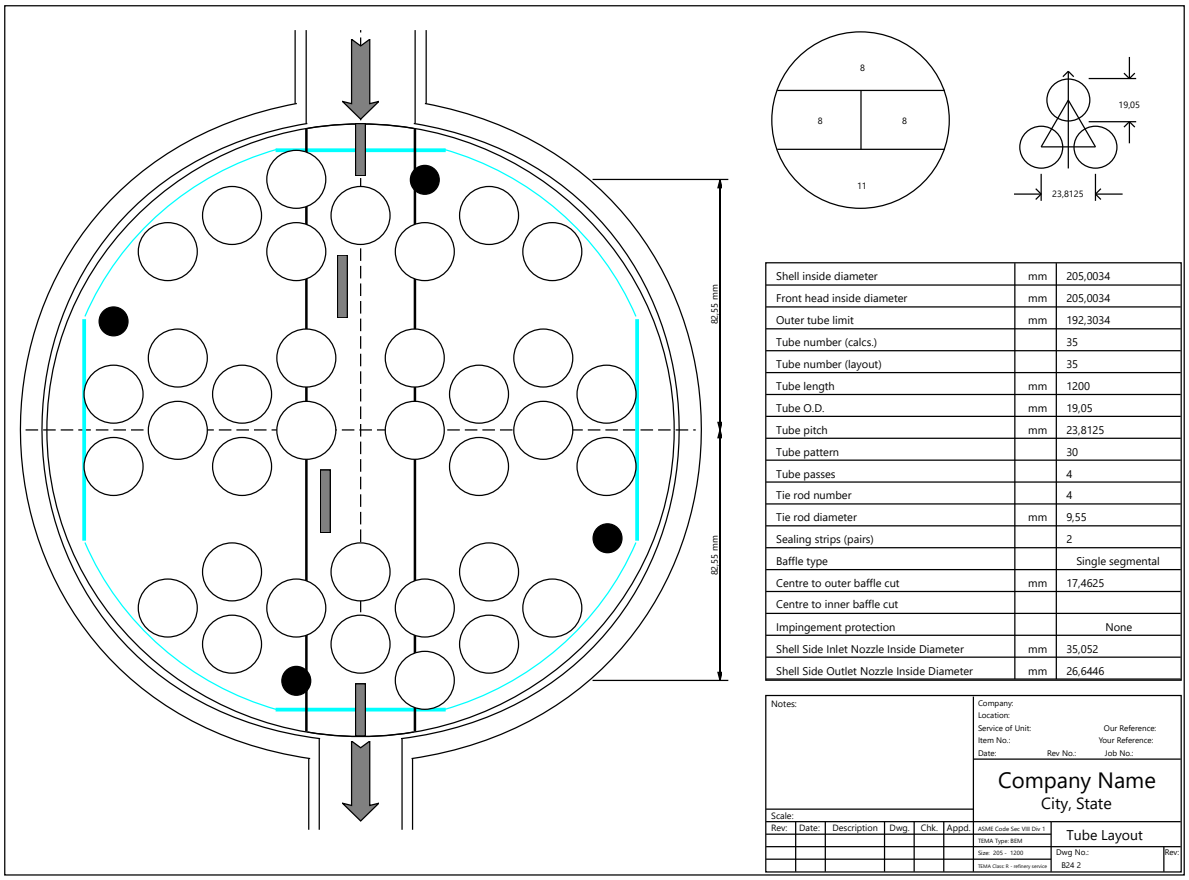

Shell inside diameter	mm	205,0034
Front head inside diameter	mm	205,0034
Outer tube limit	mm	192,3034
Tube number (calcs.)		35
Tube number (layout)		35
Tube length	mm	1200
Tube O.D.	mm	19,05
Tube pitch	mm	23,8125
Tube pattern		30
Tube passes		4
Tie rod number		4
Tie rod diameter	mm	9,55
Sealing strips (pairs)		2
Baffle type		Single segmental
Centre to outer baffle cut	mm	17,4625
Centre to inner baffle cut		
Impingement protection		None
Shell Side Inlet Nozzle Inside Diameter	mm	35,052
Shell Side Outlet Nozzle Inside Diameter	mm	26,6446

Notes:

Company:
Location:
Service of Unit: Our Reference:
Item No.: Your Reference:
Date: Rev No.: Job No.:

Company Name
City, State

Scale:

Rev:	Date:	Description	Dwg.	Chk.	Appd.

ASME Code Sec VIII Div 1
TEMA Type: BEM
Size: 205 - 1200
TEMA Class: R - refinery service

Tube Layout

Dwg No.: B24 2 Rev:

Figure 44: ASPEN model output shell & tube heat exchanger tubesheet layout.